Implantable Biological Pacemaker for Permanent Autonomous Pacing of the Heart

A Project submitted to the faculty of Worcester Polytechnic Institute

Submitted by:
Peter Chunis
John Qiao
Disha Sood
Matthew Whitman

Signatures:
_____
_____
_____
_____

Submitted to:
Professor Glenn Gaudette

Table of Contents

Table of Figures

Table of Tables

Authorship

All team members contributed equally to all aspects of the project.

Acknowledgments

Foremost, we would like to thank Professor Glenn Gaudette and Saif Pathan from BioSurfaces, Inc. for their indispensable effort, guidance, and encouragement. Additionally, we would like to thank Trevor Olsen, Lisa Wall, Chirantan Kanani, Mark Kowaleski, Catherine Lyons, and John Favreau for their constant help and guidance throughout the course of this MQP.

Abstract

Electronic pacemakers are widely used to treat cardiac pacing problems, but the devices have many inherent limitations. Pacemaking cells, which are hyperpolarization-activated cyclic nucleotide gated (HCN) transfected human mesenchymal stem cells (hMSCs), show promise as a solution to these problems, but these cells must be contained at the implant site to protect the patient and preserve functionality. This project aims to design and fabricate a device that is capable of preventing cell migration while allowing for cell-cell interactions and enabling minimally invasive delivery. A polyurethane/polyethylene terephthalate blended, micropatterned scaffold was created to achieve superior mechanical strength while maintaining low thickness necessary gap junction formation between cells. A method for heat sealing, which utilizes a 150^{o} F heating element, was devised and shown effective for completely sealing all edges of a folded flat scaffold. Migration and implant testing of the final design suggests that cells could be properly contained at the implant site without risking damage to the device caused by forces during implantation.

Chapter 1 Introduction

Implantation of permanent electronic cardiac pacemakers is a common medical procedure in the United States that effectively treats cardiac pacing problems and total failure of the heart's natural pacemaker. According to the American Heart Association, approximately 358,000 pacemaker procedures are performed annually (Roger 2010). Current pacemakers consist of a battery pack and controller, which are implanted near the right clavicle, and metallic leads, which carry electronic impulses through blood vessels from the battery pack to the patient's heart.

Though these devices cure pacing problems, their design may result in several insufficiencies that require revision surgeries to repair. Because the leads are subjected to millions of loading cycles as blood pulses around them, there is a significant risk of lead failure. Additionally, the battery pack has a finite lifespan and must eventually be replaced, and the devices are sensitive to magnetic fields so patients are restricted from MRIs and CT scans. Furthermore, re-operation is needed in pediatric patients to adjust the device to changes in body size. Finally, most permanent pacemakers are incapable of responding at all to physical and emotional stress, greatly limiting the patient's activities (Rosen et al. 2004).

Biological pacemakers are cell based pacing devices that utilize genetically modified stem cells to generate electrical pacing signals. They have the potential to help millions of people by alleviating problems and limitations created by current permanent electronic pacemakers. Previous studies have already demonstrated their effectiveness at pacemaking canine and murine models *in vitro* (Rosen et. al, 2004). Biological pacemakers would eliminate the chance of lead failure, the burden of finite battery life, limited responsiveness to physical and emotional stress of the patient, re-operations in pediatric patients, and sensitivity to magnetic fields. However, safety concerns around current biological pacemakers, which use *h*yperpolarization-activated *c*yclic *n*ucleotide gated channel (HCN) transfected human mesenchymal stem cells (hMSCs), have limited their translation to the clinic. Transfected cells may become malignant, resulting in tumor formation. In addition, these cells may wander away from the site of delivery resulting in a current density too low to continue pacing the heart. To make biological pacemakers a viable

treatment method for cardiac arrhythmias and natural pacemaker failure, a device that is implantable, prevents cell migration, and does not inhibit cell-cell interactions must be developed.

Previous studies found that an electrospun polyurethane matrix sheath with pores smaller than 3.0 μm was effective at containing hMSCs, but noted that the sheath must be thin enough to allow cells to form gap junctions through these pores. Though earlier designs effectively restrained the cells and appeared to enable gap junction formation across the membrane, the designs were not deliverable to the heart or capable of sufficient cell seeding and thus were not fully functional. The team aims to address this problem by designing a deliverable and implantable device while optimizing cell retention, gap junction formation across the membrane, and cell attachment and viability.

Chapter 2 Literature Review

Cardiovascular Disease (CVD), affecting approximately 82.6 million Americans, is the leading cause of death among both men and women in the United States. CVD also accounts for very high morbidity rates and cost in terms of disease treatment. The most common types of CVD include Coronary Heart Disease (CHD), hypertension, stroke, congestive heart failure and arrhythmias (Institute of Medicine, 2011).

2.1 Anatomy of the Heart

The heart is a hollow muscular organ that lies along the midline of two bony structures: posterior to the sternum and anterior to the vertebrae. The human heart is comparable to the size of a clenched fist, and has a tapered bottom or apex, which is located slightly to the left of the sternum. The heart is enclosed in a double-walled membrane called the pericardial sac. The outer layer of this membrane is a tough fibrous covering that helps anchor the heart and maintain its position in the chest during the cardiac cycle. The inner lining of the sac secretes a thin pericardial fluid that prevents friction between the pericardial layers during the beating of the heart (Sherwood, 2008).

The heart consists of four chambers, the upper two chambers called the atria and the lower two called the ventricles. The heart is a dual pump in which the left and right sides function as two separate pumps. The right side receives deoxygenated blood from the body and sends it to the lungs, while the left side receives oxygenated blood from the lungs and pumps it to the entire body. Since the left and right sides contain deoxygenated and oxygenated blood respectively; there exists a septum separating the two sides of the heart to prevent mixing of the blood from the left and right side. The heart contains four pressure-operated valves: the tricuspid valve which separates the right atrium and right ventricle, the bicuspid or mitral valve between the left atrium and left ventricle, the pulmonary semilunar valve between the right ventricle and the pulmonary artery, and the aortic semilunar valve between the left ventricle and the aorta. Each of these valves has a set of three flaps or leaflets, with the exception of the mitral valve, which has two. The edges of the atrioventricular (AV) valves are fastened by tough fibrous chords called

chordae tendineae, which in turn are attached to papillary muscles extending from the inner surface of ventricular walls. The chordae tendineae and papillary muscles work in unison to keep the AV valves closed during isovolumetric ventricular contraction (Sherwood, 2008).

During each heartbeat, the four chambers of the heart contract and relax in a highly synchronized and organized manner to pump blood. The right atrium receives deoxygenated blood from the body through two large veins, the inferior and superior vena cava. The deoxygenated blood then enters the right ventricle through the tricuspid valve, from where it is eventually carried to the lungs by the pulmonary artery through the pulmonary valve. The oxygenated blood is returned to the left atrium by the pulmonary vein and then flows into the left ventricle through the bicuspid valve. Finally, the oxygenated blood is pumped out of the left ventricle through the aorta and distributed to all parts of the body (Sherwood, 2008). Figure 2.1 shows the different parts of the heart and also outlines the direction of blood flow through the heart.

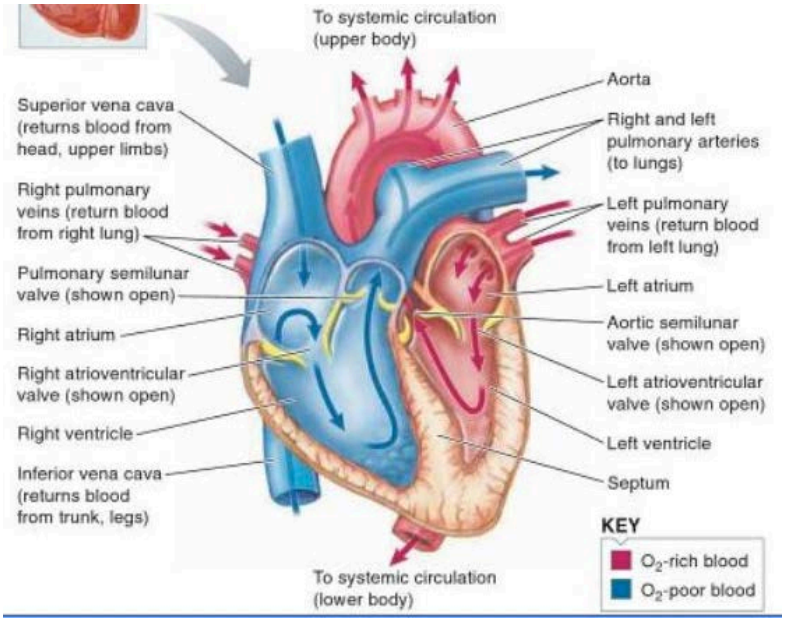

Figure 2.1: Heart anatomy and directional blood flow (Sherwood, 2008)

The heart wall is composed of three distinct layers: a thin outer layer of epicardium that covers the heart, a thin inner layer of endothelium and a middle layer of myocardium forming the bulk of the heart wall with its spirally arranged bundles of muscle fibers. The individual cardiac cells are

interconnected to form branching fibers, with the adjacent cells joined through intercalated discs. The intercalated discs consist of two types of cell-cell junctions: the desmosomes function as a mechanical connection between the adjacent cells and the gap junctions allow for action potentials to be transmitted from cell to cell. The presence of these gap junctions causes the interconnected cells to fire at the same time and contract as a single, functional syncytium. A non-conducting fibrous skeleton surrounding the valves separates the atria and ventricles, such that the atria and ventricles each form a separate syncytium (Sherwood, 2008).

2.2 Mechanical Function of the Heart

The heart is a muscular pump that continuously pumps blood between the pulmonary and systemic circulation. The mechanical activity of the heart consists of alternating cycles of diastole (relaxation and filling) and systole (contraction and ejection). Each day the heart beats an average of approximately 100,000 times (~72 beats/min), completing about 2.5 billion relaxation and contraction cycles in a 70-year lifespan. Each day, the heart pumps about 2000 gallons of blood and thus, there is 5 liters of blood in the systemic circulation at any given moment (AHA, 2011).

The directional flow of blood through the heart chambers is controlled by pressure changes generated by the mechanical activity. Moreover, the cardiac output i.e. the amount of blood pumped by the heart every minute could vary depending upon blood pressure in the blood vessels and the chambers of the heart. For a healthy adult heart, normal peak systolic and diastolic pressures are 120mmHg and 80mmHg respectively. The pressure in the atria remains more or less constant with slight variations between 0-8mmHg. Similarly, the aortic pressure is almost constant with moderate variations between the peak systolic and diastolic pressures. In contrast to the atria, the pressure in the left ventricle fluctuates dramatically between 0mmHg to slightly more than 120mmHg. This is because during diastole, the pressure in the ventricles must be lower than the atrial pressure and during systole it must be greater than the highest aortic pressure (Sherwood, 2008). Any condition, such as myocardial ischemia or infarction

due to CHD, that causes a change in these pressure distributions could result in insufficient mechanical function of the heart (Swan, 1979).

2.3 Electrical Systems of the Heart

The rhythmic mechanical pumping action of the heart is generated and maintained by the electrical activity of the heart. Heart muscle consists of two types of specialized cells: contractile cells constituting 99% of the heart muscle cells and autorhythmic cells that have pacemaker activity constituting the remaining 1% (Sherwood, 2008). Heart's normal electrical activity originates in the sino-atrial (SA) node located in the right atrial wall near the opening of the superior vena cava. The action potentials initiated in the autorhythmic cells of the SA node travel to the atria via the intermodal pathways and then through the atrio-ventricular (AV) node, bundle of His and Purkinji fibres to the rest of the heart resulting in coordinated rhythmic contraction of the different regions of the heart (Tripathi et al, 2011). Figure 2.2 shows the pathway of an excitation wave in the heart starting from the SA node.

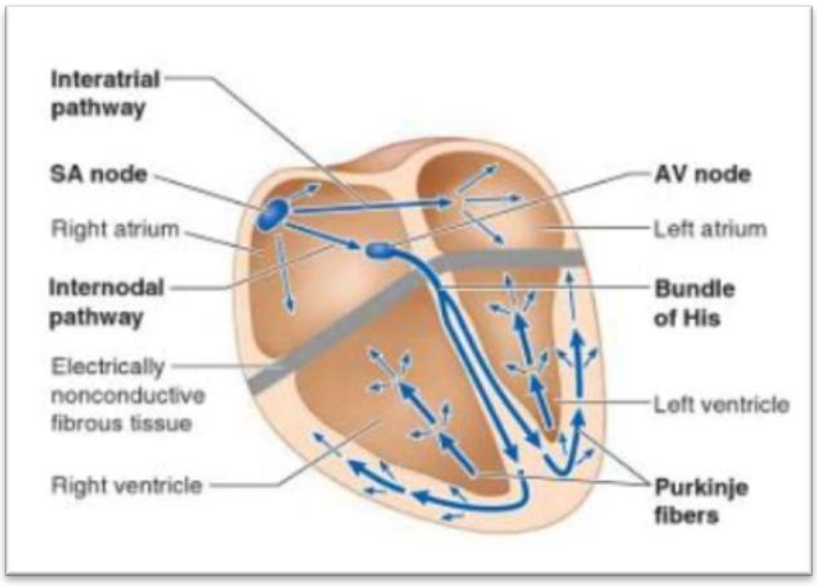

Figure 2.2: Electrical conduction system of the heart (Sherwood, 2008)

The cardiac electrical cycle is initiated and maintained by the transmembrane flux of ions via ion channels, pumps and exchangers. The specific distribution of these ion channels determines the shape of the action potential and the conductance of the excitation wave in the heart (Tripathi et al, 2011). Under

normal conditions, the heart's natural pacemaker (SA node) sets the rate of cardiac chamber contraction i.e. the heart rate. The cells of the SA node express the same genes as the contractile cells, but differ quantitatively in the expression of some ion channels, connexins, and transcription factors which generate automaticity in these myocytes (Mangoni, 2008).

The pacemaker cells of the SA node are capable of self-generating action potentials attributed to an inward current called the funny current (I_f), which is activated upon hyperpolarization in the diastolic range of voltages. The degree of activation of this current determines the frequency of action potentials causing the firing of the pacemaker cells. I_f is controlled by the levels of intracellular cAMP and thus, activated and inhibited by the ß-adrenergic and muscarinic M2 receptor activation respectively. The major constitutive subunits of f-channels in pacemaker cells are the HCN4 (Hyperpolarization-activated, cyclic nucleotide gated 4). The loss of these HCN4 subunits has been shown to cause rhythm disturbances (DiFrancesco, 2010). The strong I_f current initiated by hyperpolarization decreases the rate of K^+ efflux and increases the membrane permeability to Ca^{2+} ions. Initially, the transient type voltage-gated (T-type) Ca^{2+} channels open and once the potential reaches the threshold, the longer-lasting type (L-type) voltage-gated Ca^{2+} channels allow a large influx of Ca^{2+} ions resulting in action potential. The eventual repolarization is caused by activation of voltage-gated K^+ channels and efflux of K^+ ions. At negative potentials, there is a constant passive influx of Na^+ ions into the pacemaker cells, since these do not contain voltage-gated Na^+ channels (Mangoni, 2008). The normal rate of action potential discharge from the SA node results in 70-80 beats per min (Sherwood, 2008). Figure 2.3 shows the different phases during the action potential generation and repolarization of the pacemaker cells.

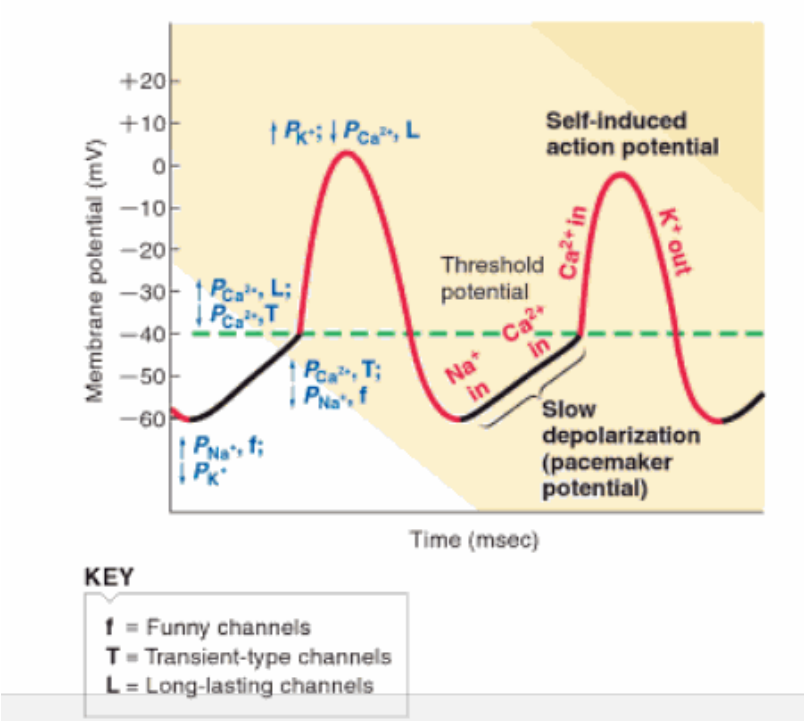

Figure 2.3: Action potential in pacemaker cells (Sherwood, 2008)

The atrio-ventricular node (AVN), a small bundle of specialized muscle cells located at the base of right atrium near the septum, ensures a conduction delay between the atria and ventricles. It also helps protect the ventricular rhythm during atrial arrhythmias. The AVN is called the secondary pacemaker since it is endowed with automaticity and can effectively drive the heart rate at about 40-60 beats per min in cases of SA node failure or block (Sherwood, 2008). The Bundle of His is a tract of specialized cells originating in the AVN that enters the interventricular septum and branches into left and right bundle branches. At the apex of the heart, the Bundle branches contact the Purkinji fibers, which extend from the Bundle of His allowing for the fast propagation of an excitation wave generated upstream throughout the ventricular myocardium. The Bundle of His and Purkinji fibers can also pace the heart at the rate of 20-40 beats per min if the conduction in the AVN is blocked (Mangoni, 2008).

Unlike the autorhythmic cells, the action potentials of the contractile cells are initiated by the electrical activity propagated from the pacemaker cells. This activity cause the resting membrane potential (-90mV) of the contractile cells to rise rapidly due to the opening of the voltage-gated Na^+ channels and consequently large influx of Na^+ ions. The rapid depolarization causes an action potential

and is followed by a two-phase repolarization. The initial plateau phase of repolarization is maintained by a slow influx of Ca^{2+} ions through the L-type Ca^{2+} channels, while the rapid falling phase is caused by the increase in K^+ efflux due to the opening of voltage-gated K^+ channels (Sherwood, 2008). These phases of depolarization and repolarization can be seen in Figure 2.4.

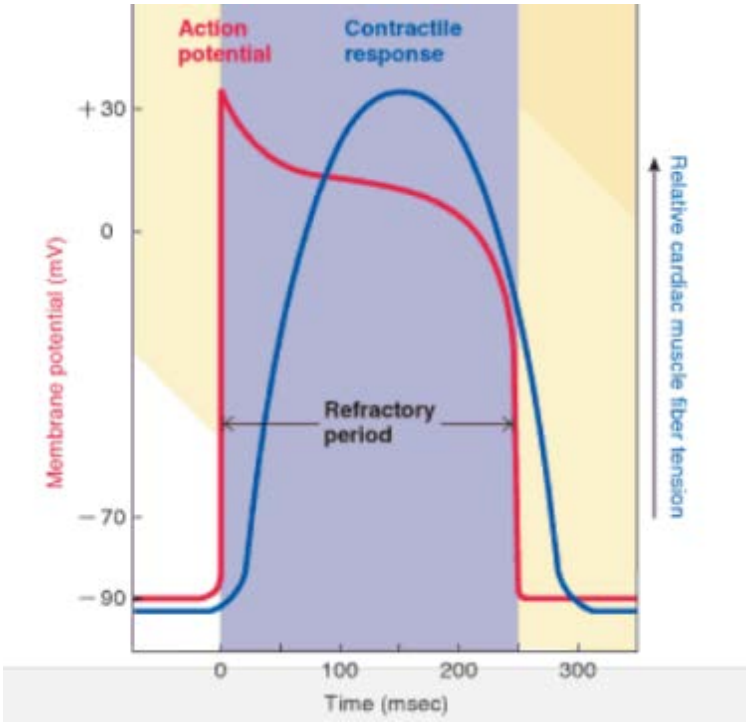

Figure 2.4: Action potential and conctractile response in cardiomyocytes (Sherwood, 2008)

The electrical currents generated by the pacemaker cells that spread to all the contractile cells throughout the heart during depolarization and repolarization can be recorded on the body surface to produce an electrocardiogram (ECG). The P wave of the ECG represents atrial depolarization, the QRS complex represents the ventricular depolarization and simultaneous atrial repolarization and the T wave represents the ventricular repolarization. Any abnormalities in the heart rhythm can be detected by the deviations observed in the different segments of an ECG recording (Sherwood, 2008).

2.4 Arrhythmia

Cardiac arrhythmias, a type of heart disease involving an abnormal heart rhythm, can result from alterations in the SA node pacemaker activity or a blockage of electrical conduction downstream of the SA node. Arrhythmias can also result from the formation of a group of hyperactive cells called an ectopic

focus that fire at a rate greater than the SA node pacemaker cells (Sherwood, 2008). Brief arrhythmias do not affect the heart adversely, but prolonged arrhythmias could result in inefficient pumping of blood. Arrhythmias can be of different kinds: bradycardia is insufficient beating of the heart (less than 60 beats/min); tachycardia is rapid beating of the heart (more than 100 beats/min); atrial fibrillation or quivering, which is characterized by rapid, irregular, uncoordinated depolarizations of the atria; or ventricular fibrillation or fluttering involving uncoordinated, chaotic contractions of the ventricles. Figure 2.5 shows the difference between a normal heart rhythm and the heart rhythm during tachycardia. If left untreated, most arrhythmias could lead to heart failure (AHA, 2011). Currently, such arrhythmias are treated by implantation of electronic pacemakers in the patients. In the United States alone, approximately 358,000 electronic pacemakers are implanted every year. Almost all the pacemakers implanted are to treat bradycardia (Wood, 2002).

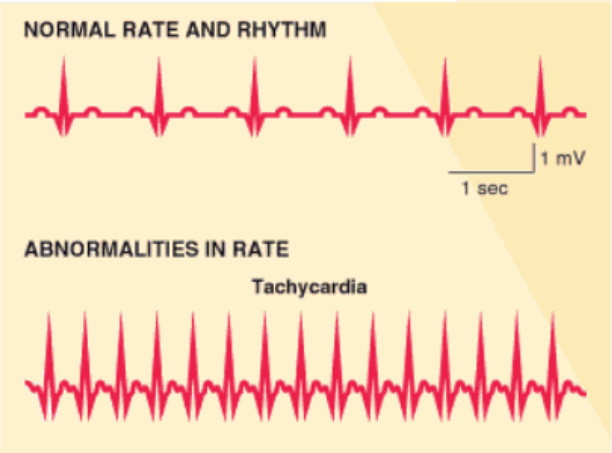

Figure 2.5: ECG Signals (A) Normal PQRS wave (B) Rapid HR during tachycardia (Sherwood, 2008)

2.5 Electronic Pacemakers

The typical electronic pacemaker consists of two parts: the pacemaker unit and the wires that connect the pacemaker to the heart. The pacemaker unit consists of a battery and a controller, which monitors the patient's underlying heart rhythm and accordingly delivers electrical signals at the required rate. The electronic pacemakers can either be single chamber, consisting of only a single wire connected to the heart, or dual chamber with two separate wires connected to the upper and lower heart chambers. The implantation of the pacemaker system is done under normal anesthesia with the pacemaker unit being

placed under the skin below the collarbone and the wires are placed through a blood vessel beneath the collarbone. The wires are properly positioned in the blood vessels using X-ray and finally connected to the pacemaker unit. The implantation surgery typically takes around 1-2 hours and the risk of complications is about 1-2%. Electronic pacemakers enable efficient pacing of the heart without any major disruptions to the patient's mobility or daily activities (Wood, 2011).

However, these pacemaker systems do present a number of limitations for long-term cardiac pacing. The main problems include replacement of generators due to limited battery life and problems associated with leads like fracture, displacement, inappropriate stimulation, loss of insulating material, or tissue perforation. All these disadvantages are exacerbated in the case of pediatric patients due to physical development and tissue ingrowth. Other possible complications include infection, thrombosis, maladaptive cardiac remodeling and lack of autonomic neurohumoral responsiveness (Cowan, 2011).

2.6 Biological Pacemakers

Electronic pacemakers are an effective treatment option for people with sinoatrial (SA) node dysfunction. However, with their numerous limitations, electronic pacemakers are perceived only as a treatment rather than a cure. (Cohen et al, 2005). Repeated operations are required to elongate and reposition the leads in pediatric patients. In addition, the risk of heart failure may increase with long-term pacing (Freudenberger et al, 2005).

In a healthy heart, the SA node is the main biological pacemaker, in which all ion channels and transporters needed to pace the heart reside in the sinoatrial nodal myocytes (Cohen et al, 2005). The SA node also exhibits other important characteristics such as, the localization and congregation of SA node myocytes, strong mechanical and electrical integration into the cardiac tissue, the ability to initiate action potentials that are sufficient to propagate and regulate the rhythm of the heart, and capability to generate rhythm in the heart that responds to the physiological and emotional changes of the body (Rosen et al, 2004). The intrinsic characteristics of the SA node serve as fundamental guidelines for the designing of biological pacemakers.

Based on the characteristics of the SA node and the limitations, the perfect biological pacemaker should satisfy a number of criteria. The biological pacemaker should be able to generate stable and spontaneous rate at physiological acceptable rate, it should be self-sustaining and require no battery or electrodes, it should pose no risks of inflammation and tumor growth at the implantation site, it should be immobilized at the implantation site and requiring no future replacement, it should have the ability to respond to changing philological and emotional demands of the body, and it should be at least as effective and reliable as electronic pacemakers (Rosen et al, 2004).

In order to present a cure to cardiac rhythmic conditions, different types of biological pacemakers are proposed to mimic the natural cardiac pacemaker and to overcome the limitations and risks associated with electronic pacemakers. A number of strategies can be implemented to initiate pacing of the heart including, up-regulating β-adrenergic responsive, decreasing outward current (I_k), increasing inward current (I_f), and introducing new pacemaker cells to the heart (Anghel, 2007). Some strategies are not widely adapted due to their underlying disadvantages. The up-regulated β-adrenergic receptors demonstrated higher heart rate during *in vivo* testing. However, the overexpression of β-adrenergic receptors lacks long lasting effect, and the β receptor over expression may lead to other negative effects in the heart (Rosen et al, 2004). The down-regulation of the outward current also has a number of limitations including prolonged action potential and irregularities in cardiac rhythms. The strategy to increase inward current has been extensively studied because the method poses no effect on prolonging the action potential duration, and the inward current is well regulated by the autonomic nervous system (Qu et al, 2003). Finally, the stem cell approach is to differentiate new pacemaker cells to exhibit the aforementioned characteristics.

Three methods were formulated to create and deliver a biological pacemaker, such as the injection of naked DNA, viral vectors, and cells into the heart (Cohen et al, 2005). HCN (hyperpolarization-activated, cyclic nucleotide-gated) gene is used to overexpress the inward depolarizing current (I_f). Direct exposure of naked DNA to the cardiac myocytes yields insufficient up-take rate and short duration. Introducing viral vectors carrying the gene demonstrated much higher transfection

efficiency. However, depending on the type of viral vectors used, they may cause immune response or tumor growth in the body. The use of cells as carriers of the gene presents itself as a safer option as the genes are inserted using electroporation *in vitro*.

2.7 HCN Transfected hMSCs as a Biological Pacemaker

As a proof of concept, canine studies have demonstrated the effectiveness of HCN transfected myocytes in generating atrial beats via injection of adenovirus containing the gene into the heart (Qu et al, 2003). By transfecting stem cells *in vitro*, the risks associated with viral vectors can be avoided. Having the ability to differentiate into multiple cell types such as bone, cartilage, muscle, tendon, and fat, mesenchymal stem cells are chosen for the biological pacemaker application for their multipotency. Adult mesenchymal stem cells are also desirable because they are readily available and abundant in adult patients. Typically harvested from bone marrow, adult mesenchymal stem cells can be obtained from many parts of the body. In clinical applications, these cells are also immunoprivileged, meaning they provoke minimal immune response from the host body (Rosen, 2004). Combined with their low immunogenicity and high availability, adult human mesenchymal stem cells have the potential to provide an off the shelf cure for SA node dysfunction. For patients who are not suitable to receive allogeneic cells, the mesenchymal stem cells could also be obtained from the patient's own marrow.

Adult human mesenchymal stem cells have demonstrated consistent ion channel properties. In addition, these cells are also shown to form functional gap junctions among themselves and with cardiomyocytes both *in vivo* and *in vitro* (Rosen, 2007). Given their multipotency, immonoprivileged nature, good availability, and gap junction formation with neighboring cells, adult mesenchymal stem cells are accepted as a promising platform for gene therapy.

Rosen et al explored the use of adult human mesenchymal stem cells transfected with HCN genes for a biological pacemaker (2007). A normal sinoatrial nodal pacemaker cell is able generate its own depolarization and initiate an action potential that can be propagated to neighboring myocytes through gap junctions. The flow of action potential continues to flow throughout the heart and results in the

controlled contraction of the atria and ventricles. Whereas, in an adult mesenchymal stem cell that is transfected with the HCN gene, the inward current in the stem cell caused by the high resting potential of the adjacent myocytes would initiate a current flow to the adjacent myocytes, which ultimately depolarize and generate an action potential. This action potential is then propagated down the conducting system of the heart (Rosen et al, 2007). Essentially, the HCN transfected stem cell and adjacent myocytes act together as a pacemaker unit, as shown in Figure 2.6. Unlike the natural pacemaker, the HCN transfected adult mesenchymal stem cells would not generate spontaneous heart rates by itself because it only functions as a source of depolarizing current to the neighboring myocytes, which generates the action potentials required to pace the heart. The advantage of allowing the genetically modified stem cell and its adjacent myocyte to function synchronously as a single pacemaker unit is that no further work is needed to fully differentiate the stem cell into a pacemaker cell.

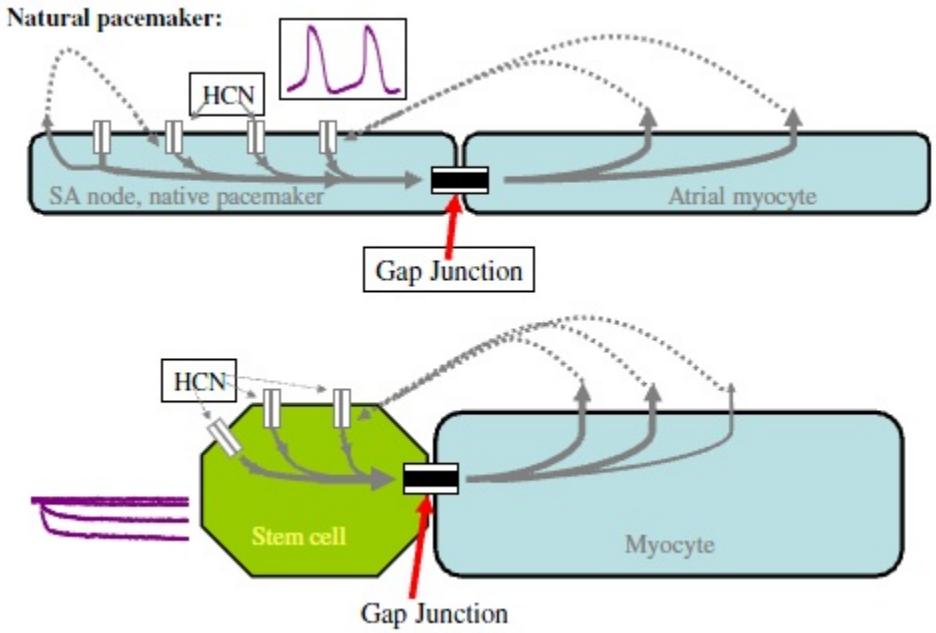

Figure 2.6: hMSC vs. native pacemaker. (A) SA nodal cell working as a pacemaker unit. (B) HCN Transfected hMSC and cardiomyocyte working as pacemaker unit (Rosen, 2004).

The performance of HCN transfected adult human mesenchymal stem cells is evaluated using *in vitro* and *in vivo* models (Rosen et al, 2004). In practice, the HCN gene has a transfecting efficiency of around 40% using electroporation, which temporarily permeabilize the cell plasma membrane with an

external electrical field and allows the uptake of genetic material (Potapova et al, 2004). For the *in vitro* model, adult mesenchymal stem cells are transfected with either HCN gene plus a fluorescent marker (GFP) or GFP alone. The cells are then introduced to a monolayer of neonatal rat ventricular myocytes. After the formation of functional gap junction coupling, the myocytes in contact with the stem cells containing both the HCN and GFP beat significantly faster than the myocytes in contact with the stem cells expressing GFP alone, as shown in Figure 2.7 (Rosen et al, 2004). *In vivo* model testing of the function of the HCN transfected adult mesenchymal stem cells using canine studies also yielded similar results. In dog hearts that were injected with stem cells expressing both HCN and GFP, a higher average heart rate was recorded, originating from the injection site. On the other hand, dogs that received stem cells expressing GFP alone demonstrated a considerably lower average heart rate, originating from multiple locations in the heart (Rosen et al, 2004).

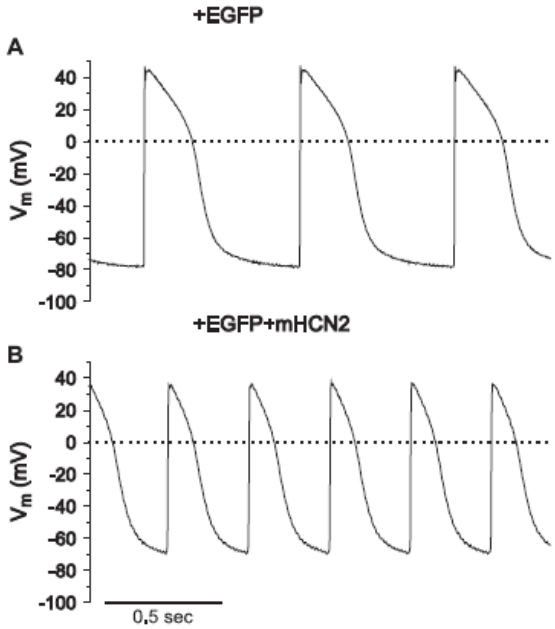

Figure 2.7: Action potentials of normal hMSCs (Top) and HCN2 transfected hMSCs (Bottom). The transfected cells beat much faster (Rosen, 2004).

Although HCN transfected adult human mesenchymal stem cells demonstrate efficient pacemaker function with great clinical and commercial benefits, a number of major concerns remain to be addressed before they become viable treatment. Due to the natural characteristics of the stem cells, there is a risk of tumor growth, cell migration, and differentiation into other cell types in the long term (Rosen, 2004).

These limitations not only reduce the pacemaker functions of the HCN transfected stem cells, they also pose serious health risks to the patients.

2.8 Electrospun Scaffold

To overcome the limitations of HCN transfected adult human mesenchymal stem cells, electrospinning can be used to create an scaffold that inhibits cell migration, maintains pacemaker function, and reduces the danger of tumor growth. Electrospinning is an efficient and inexpensive manufacturing process that involves the use of a high electric force to extract a nanofiber from a charged capillary tip onto an oppositely charged colleting plate or drum, as shown in Figure 2.8 (Khil et al, 2003). Electrospinning is capable of producing a highly porous nanofibrous scaffold with good structural integrity (Pedicini, 2003). For use in a biological pacemaker application, the electrospun matrix must have appropriate surface thickness and porosity to allow for the formation of gap junctions across the scaffold surface and the prevention of cell migration. The electrospinning process allows for fine controls of different parameters of the scaffold such as fiber diameter, thickness, and mesh pore size by altering polymer solution concentration, applied voltage, working distance, and spin time (Khil et al, 2003).

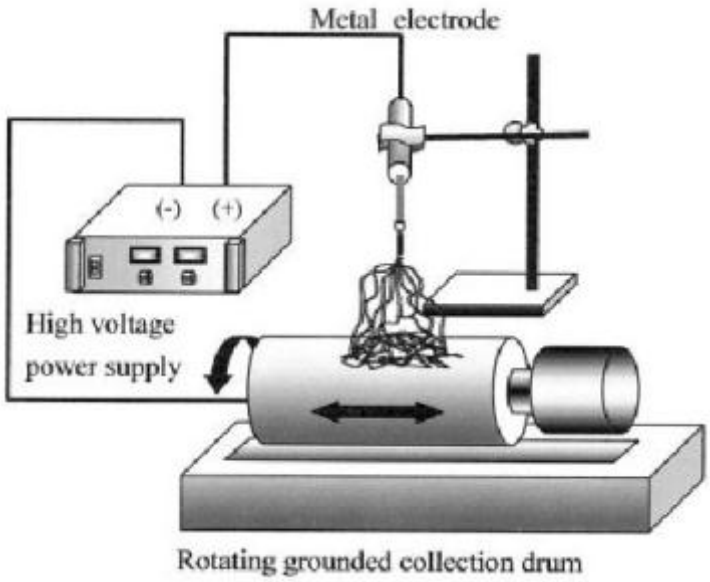

Figure 2.8: Schematic of electrospinning apparatus (Khil et al, 2003).

A range of polymers can be used to make electrospun scaffolds. Polyurethane is widely used in production of tissue engineering scaffolds due to its good biocompatibility, manufacturability, mechanical properties, and wear resistance. With good permeability to oxygen and water, polyurethane can maintain adequate diffusion of nutrients to cells *in vivo* (Khil et al, 2003). However, additional structural support is required for an electrospun polyurethane matrix with the desirable thickness for biological pacemaker applications.

Chapter 3 Project Approach

Before we could begin our testing and evaluation, we needed to define our design parameters and formulate a plan. This was accomplished through establishing objectives and constraints, identifying functions and specifications, and finally revising our client statement. With all of these parameters defined, we could proceed to testing and design validation.

3.1 Initial Client Statement

Based on the information gathered from our background research, we developed an initial client statement:

> To create a biocompatible scaffold that would inhibit migration of hMSCs while allowing for gap junction coupling with native cardiomyocytes. The device should also be easy to deliver.

Through discussions with our advisor and client, we developed a list of objectives and constraints that would help us meet our project goals.

3.1.1 Objectives

The first parameter we needed to establish was design objectives. We defined "objective" as an aim or end of an action; something towards which effort is directed (Dym, Little, Orwin, & Spjut, 2009). With this in mind, we were able to formulate numerous objectives for our design.

Our design should be safe for the user, patient, and cells. It should not have any sharp objects protruding outward, ensuring the safety of the user and the patient. Additionally, it should limit cell migration to prevent loss of current density or tumor formation away from the implant site. The device must also be permeable to nutrients and cannot be cytotoxic.

The device should form gap junctions between all the cells present in the device and native cardiomyocytes. Gap junctions allow for ions to freely pass from cell to cell. In the case of the heart, gap

junctions allow smooth and synchronized pacing to occur. Therefore, gap junction formation is essential to the functionality of our device.

Cells should be adhered to the device for delivery and implantation. This ensures patient safety as well as reliability of the device. If the cells are loose on the surface of the device, they could fall off during delivery or wander once implanted. This could lead to tumor formation or decrease the cell density on the device's surface resulting in insufficient current density to pace the heart.

Ideally, there should be no synthetic divider between the hMSCs and the native myocytes. However, the device should not degrade until the hMSCs are completely immobilized so as to ensure stability in the connections between native and foreign cells. Additionally, wandering cells have the potential to be hazardous, so immobilization must be guaranteed. Thus, the device should last a substantial amount of time, before degrading.

Cyclic pulsing of the heart creates stresses that could result in fatigue failure of the device. The device must withstand normal cardiac forces and cyclic loading without greatly hindering normal mechanical and electrical function within the tissue.

Since the device is meant to pace the left ventricle, it must fit into either the ventricular septum or the left ventricular wall. Assuming that the heart is about the size of the human fist, the septum should be about 10cm in length and about 8mm in thickness. This means the device must be less than 8 mm long to prevent perforation of the septum during implantation. The ventricular wall is approximately 2-3 mm thick, so the device must be less than 2 mm long to prevent perforation of the heart wall. The attached cells will receive signals from the healthy native cells and restore normal pacing to the heart. Much of the data presented here is based on unpublished research conducted by Glenn Gaudette and his collegues. The data here is meant to serve as a rough average size rather than an absolute result. There is room for fluctuations and variances between patients. Other desirable objectives include a reasonable shelf life and ease of use.

3.1.2 Constraints

One of the most pressing constraints on this project is cost. All expenses associated with design, budget of $616. Additionally, the project must be completed March 2nd, 2012. Completion by this deadline will ensure that there is ample time to prepare the final product for presentation.

For the device to be worth using, it must be biocompatible and have low immunogenicity. Immune response, strong inflammatory response, or fibrotic encapsulation could all impede the pacemaker unit from functioning properly in situ.

The device must also stop the cells from migrating to other parts of the body. It must create gap junctions between native and implanted cells, and must be implantable within the myocardium. The final step of planning involved mapping functions to satisfy the objectives and constraints, and determining means for achieving those functions.

3.1.3 Functions

To meet the defined objectives, the cells must adhere to the surface of the device, form gap junctions, and immobilize cells as described in the objectives section. Additionally, the electrospun matrix must promote cell viability to minimize cell density loss between seeding and implantation of the device. The device must be able to withstand the forces within the heart while minimizing the decrease in cardiac function. It must be implantable into the ventricular septum or left ventricular wall to enable gap junction formation between hMSCs and native cardiomyocytes.

3.1.4 Specifications

This section defines to device requirements quantitatively. A literature review determined that the optimal minimum cell count for a biological pacemaker is about 300,000 (Potapova et al, 2004).Using this number and cell density data collected in the lab using normal hMSCs, we determined a device cross-sectional area of 12mm x 12mm to be sufficient for reaching 300,000 cells per device. To confirm functionality of the device, we will expect to see gap junction formation within the first 48 hours after

implantation. Taking into consideration all of the objectives, constraints, functions, and specifications, we could start planning on how we want to fabricate this device.

3.2 Function Means Tree

A function means tree was used to visually map possible approaches to accomplishing the necessary functions. The functions mean tree is shown in Appendix C.

3.3 Ranking of Design Requirements

An objectives tree, shown in Appendix B, was used to visually assess the objectives of the design as well as the subcomponents of each objective. This tree enabled the team to better understand the problem, which enabled us to tailor our design to the intricacies of the problem. After constructing the objectives tree, the first degree objectives were ranked (intellectual property, ease of use, easily implantable, etc.) using a pairwise comparison chart. Only first degree objectives that fell under the same primary objectives (safety, marketable, reliable, and functional) were ranked against each other.

The charts were made with the primary objectives on both the vertical and horizontal axis. Each objective on the vertical axis was ranked against the objective in the horizontal axis with a 1, 0, or ½. A box marked with a 1 indicates that the objective on the vertical axis is more important than the horizontal axis; A 0 indicates that the objective on the horizontal axis was more important than the vertical axis, and a ½ indicated that both objectives were equally important. The charts can be seen in Tables 3.1 to 3.4.

Table 3.1: Safety Pairwise Comparison Chart

Safe	User	Patient	Cells	Score
User				
Patient				
Cells				

Table 3.2: Marketability Pairwise Comparison Chart

Marketable	Cost	Ease of Use	Shelf Life	First to Clinic	Intellectual Property	Score
Cost						
Ease of Use						
Shelf Life						
First to Clinic						
Intellectual Property						

Table 3.3: Reliability Pairwise Comparison Chart

Reliable	Structural Integrity	Failure Rate	Score
Structural Integrity			
Failure Rate			

Table 3.4: Functionality Pairwise Comparison Chart

Functional	Gap Junction	Cell Adhesion	hMSC Immobilization	Encase Cells	Easily Implantable	Close to Myocardium	Manufacturing Feasibility	Score
Gap Junction								
Cell Adhesion								
hMSC Immobilization								
Encase Cells								
Easily Implantable								

Close to Myocardium								
Manufacturing Feasibility								

The completed tables from the four team members and the client were tallied and put into Table 3.5.

Table 3.5: Pairwise Comparison Results

Safety		**Functional**		**Reliable**		**Marketable**	
Objective	**Score**	**Objective**	**Score**	**Objective**	**Score**	**Objective**	**Score**
Patient	9	hMSC Immobilization	18.5	Structural Integrity	3.5	Ease of Use	13.5
Cells	4.5	Gap Junction Formation	17.5	Failure Rate	1.5	IP	12.5
User	1.5	Close to Myocardium	14.5			First to Clinic	9.5
		Manufacturing Feasibility	10.5			Shelf Life	8.5
		Cell Adhesion	10			Cost	6
		Encase Cells	7				
		Easily Implantable	3				

3.4 Revised Client Statement

The information gathered during the planning stages was used to revise our initial client statement. Using our objectives, constraints, functions, and specifications, a revised client statement was created:

> To create a biocompatible device to deliver hMSCs that would inhibit the migration of hMSCs while allowing for gap junction coupling with native cardiomyocytes. The device should also be fairly easy to deliver and must promote cell adhesion to the device surface. Implanted hMSCs must be immobilized at the implant site and must pace native myocytes. A minimum scaffold surface area, to be determined through experimentation and cell viability, must be achieved in order to produce sufficient cardiac pacing. The device should also provide sufficient mechanical support to withstand cardiac forces and maintain cell viability. It must also be implantable within close proximity of native myocytes while minimizing decrease in mechanical function and maintaining natural conductivity in the heart.

Chapter 4 Alternative Designs

For the purposes of determining a proper design to satisfy the desired functions and objectives, 7 preliminary designs were devised. These designs were evaluated on several criteria to determine 2 alternative designs. Finally, these alternative designs were compared to determine 1 final device design.

4.1 Needs Analysis

In order to provide ourselves with multiple functional designs for testing, we closely examined the revised client statement, objectives, constrains and functions of the project. Regardless of the effectiveness and efficiency of the designs, all designs of the device must satisfy the project constraints. As mentioned in chapter 3, the designs must be cost effective, safe for the patients and the users, sufficiently compact to be implanted into the heart, allowing the formation of gap junction coupling, and preventing cell migration.

From the pairwise comparison chart, the team rated each of the primary functions that the pacemaker device should satisfy. After compiling all the scores, hMSC immobilization is deemed the most important among all the primary functions. With device safety being our most important objective and constraint, the immobilization of hMSCs is the corresponding function that ensures the safety of the device for the patients. This function arises from the basic limitations of using HCN transfected hMSCs for pacing. Chapter 4 extensively explained the safety concerns of using stem cells for pacing. Compared with conventional electronic pacemakers, the use of stem cells in pacing has the potential risks of rejection, inflammation, tumor growth, cell migration, and uncontrolled differentiation into other cell types. Therefore, every design should not allow any cell migration for the safety of the patients.

Formation of gap junctional coupling is evaluated as the second most important function for the biological pacemaker. It is the most important function other than safety because function gap junction formation is required by the HCN transfected hMSCs for pacing of a heart. Specifically, Rosen et al found that gap junctional coupling between the stem cells and the surrounding myocytes must be sufficient to depolarize the adjacent myocytes (2004). Therefore, there is no optimal percentage of gap

junction formation, the more the gap junctional coupling; the more efficient and effective the pacemaker unit would be.

Rosen et al demonstrated that HCN transfected hMSCs injected into the canine hearts initiated action potential from the injection site only, and propagated throughout the heart for pacing (2004). Since myocardium is the tissue that is responsible for contraction of the ventricles, it is determined that the biological pacemaker should be implanted as close to the myocardium as possible. Consequently, the design of shape, size, and mechanical properties of the biological pacemaker scaffold are extensively affected by this function.

Manufacturing feasibility, cell adhesion, cell encasement, and ease of implantation are the other primary functions that the pacemaker should satisfy. Among these, manufacturing feasibility is deemed to be the most important because it determines the cost and the feasibility of the entire design. This function also affects the shape and complexity of the scaffold design. Lastly, easily implantable was determined to be the least important primary function. With this novel method of using stem cells for pacing of the heart, the device design should ensure effectiveness and efficiency before allowing for easy implantation for the surgeons.

Two delivery methods were also examined for the ease of delivery of the biological pacemaker. One method was the suture based delivery method, in which a surgical suture needle would be used to guide the insertion of the biological pacemaker. Prior to delivery, one end of the scaffold would be heat shrink to the blunt end of the needle. The second method would be the catheter based delivery method, in which a catheter designed previously by an MQP group for the delivery of microthreads would be used. Similar to the delivery of microthreads, the biological pacemaker would be draped over the inner core for easier insertion. As shown in Figure 4.1., after the outer needle is inside the myocardium, the outer needle would be pulled back while the inner core deploys the biological pacemaker. The catheter based delivery mechanism was designed to reduce shear on the scaffold as it passes under and through the myocardial surface (Costa et al, 2011).

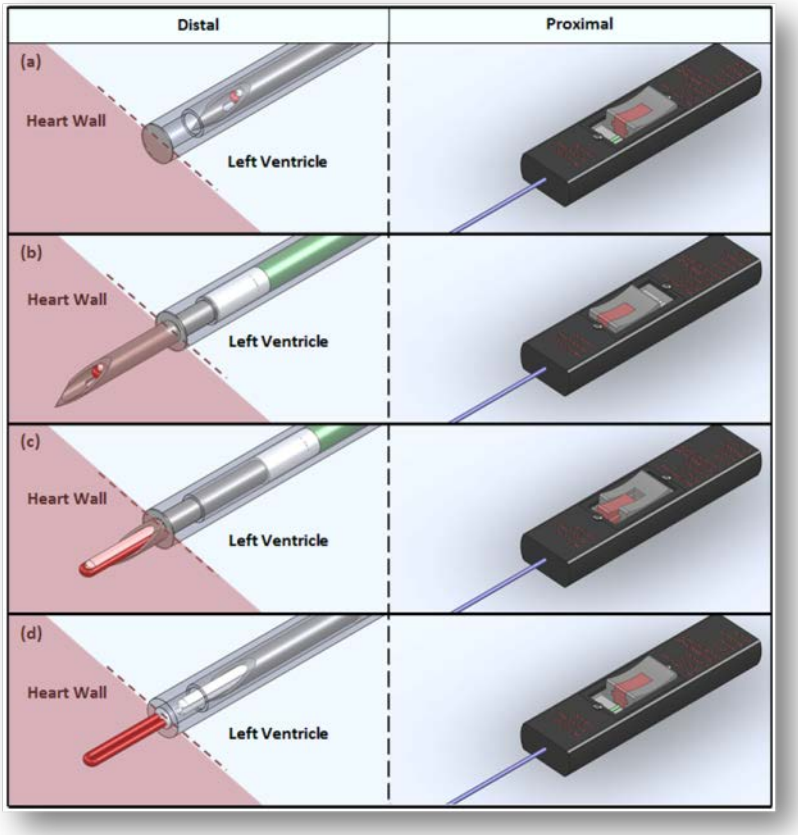

Figure 4.1: Staged deployment of catheter (Costa, 2011)

4.2 Preliminary Designs

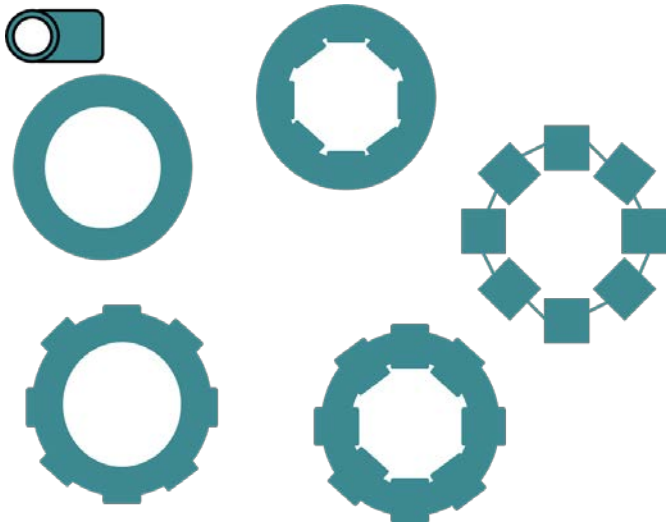

Figure 4.2: Preliminary Design 1

Preliminary design 1 focuses on a doughnut-like cylinder with a hollow, or open, core. The top left design is a basic circular design where the cells would be seeded in the blue ring region. The bottom left and top middle designs are almost identical to each other. The only difference between the two is the positioning of the “teeth” represented by the eight rectangular protrusions on the outside and inside of the ring, respectively. The bottom right design combines the previous two designs to create better fixation. The far right design is a spinoff of the bottom right design. The only difference is that the ring region will not seed the cells, but instead act as support for the chambers of cells.

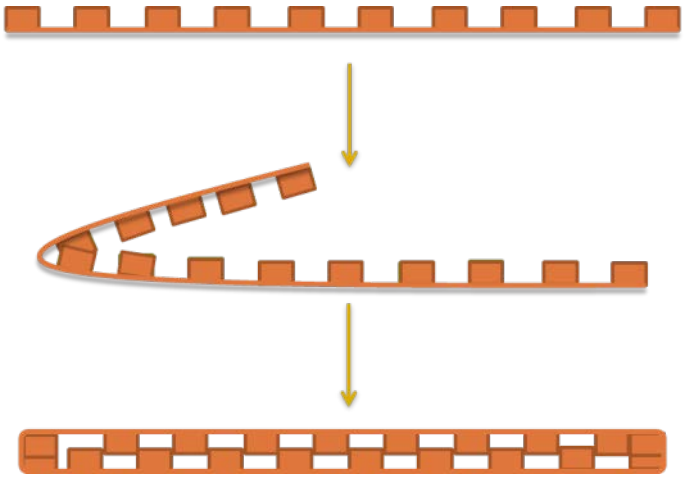

Figure 4.3: Preliminary Design 2

Preliminary design 2 is consisted of supporting rods aligned in a unidirectional arrangement on a sheet of porous scaffold. The rods can be placed on the collecting plate before the electrospinning process. As a result, electrospun nanofibers should accumulate directly on top of the rods. Next, HCN transfected hMSCs could be seeded on either side of the sheet. The sheet would then be folded into a rectangular shape after cell attachment, sandwiching the cells in the middle. The edges could be sealed using heat shrink.

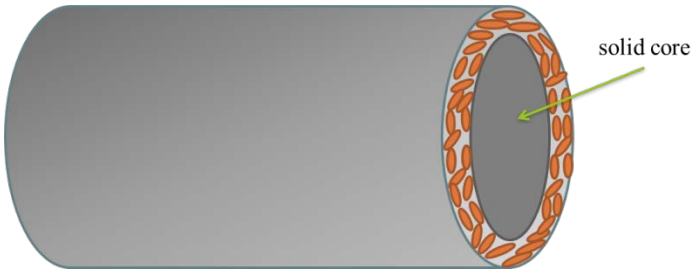

Figure 4.4: Preliminary Design 3

Preliminary design 3 is consisted of a tubular construct outer layer and a solid inner core. The outer layer can be easily made using electrospinning with a collector drum. Due to the flexibility in the fabrication technique, the inner and outer diameter of the tubular construct can be easily controlled and altered. The cells would be seeded in the empty space between the two layers. The two ends would be sealed using heat shrink. The tubular shape of this design allows for easier insertion into the myocardium when compared with the rectangular design.

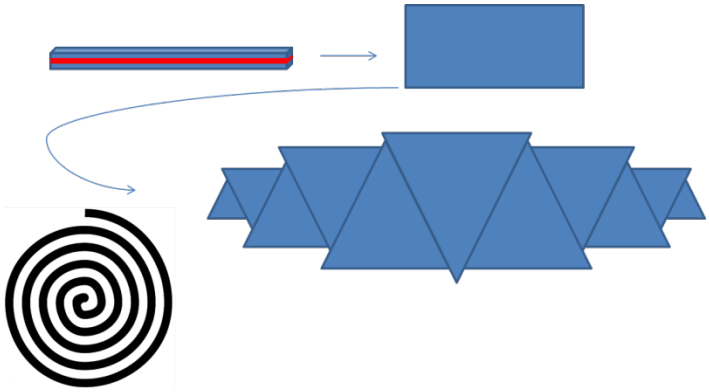

Figure 4.5: Preliminary Design 4

Preliminary design 4 is a combination of previous two designs. Due to low seeding density within the tubular construct, the cells would be seeded on a flat sheet of porous scaffold. After cell attachment, the sheet would be rolled into a tubular shape for ease of implantation.

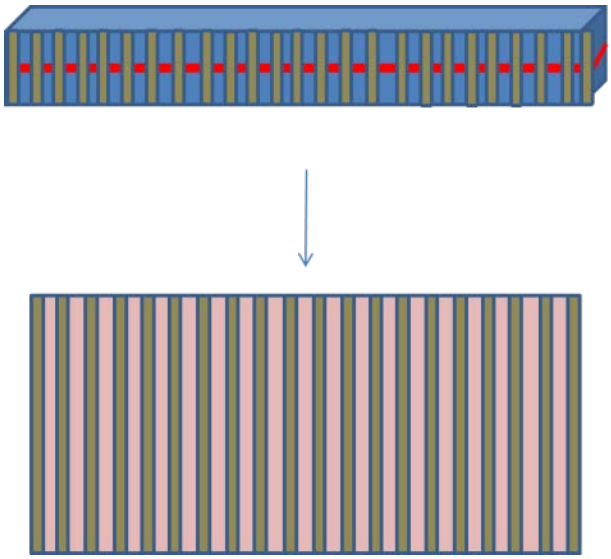

Figure 4.6: Preliminary Design 5

Similar to preliminary design 2, this design is another rectangular shaped scaffold that allows for high seeding density on a flat surface. Supporting rods are aligned between the two layers of the scaffold for structural integrity and structural support. Heat shrink can be used to seal the four edges of the device before implantation.

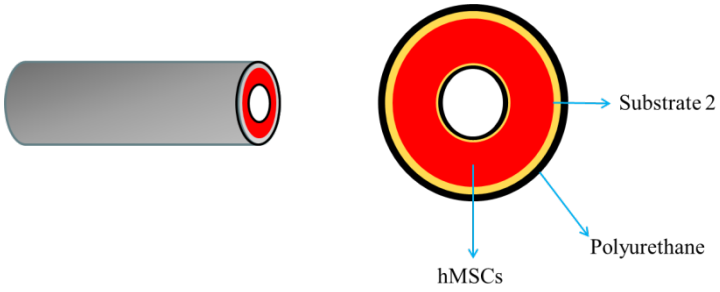

Figure 4.7: Preliminary Design 6

Preliminary design 6 is a spinoff of design 1. It is a much more complicated design where the ring region can be broken down into three different layers. The first layer is the outer layer (indicated in black). This is composed of polyurethane and would give the device structural support. The second layer is the middle coating (indicated in yellow). This would be a coating of some polymer that would promote cell adhesion to the device. The final layer is the cell seeding region (indicated in red). This is where the cells would be seeded and, hopefully, stay immobilized thanks to the coating.

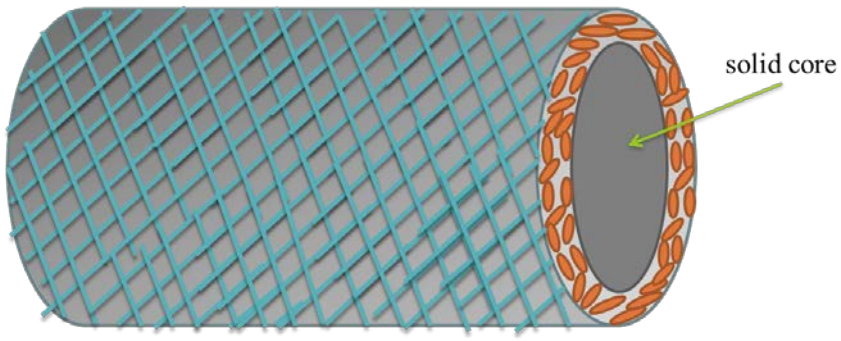

Figure 4.8: Preliminary Design 7

Preliminary design 7 incorporates the structural rigidity of the rod-supported designs with the ease of implantation of the tubular design. The outer scaffold contains a mesh-like backbone for mechanical support. The internal metallic mesh can be installed to the collector drum. During electrospinning, nanofibers are then layered on top of the mesh to create a porous scaffold.

4.3 Alternative Designs

Based on the results of our initial feasibility studies pertaining to our preliminary designs, we narrowed down to two alternative designs. These alternative designs are essentially a modification of the preliminary designs 5 and 7 as shown in chapter 4.

Alternative Design 1 is a modification of the preliminary design 7. This design will involve a cylindrical mesh-like fibrin support structure, which would be pre-made and installed on the small diameter collecting drum before electrospinning the scaffold material onto it. During electrospinning, the PE/PU fibers will be layered over the fibrin mesh to create a porous scaffold. The resulting scaffold once removed from the mandrel and processed further according to the existing protocol, by placing in the water and ethanol baths, would retain its added structural integrity provided by the fibrin support structure. The core of this scaffold will be hollow and cells will seeded onto inner circumferential areas. Once the cells are seeded along the entire surface area, the ends would be sealed using a custom heat shrink method. The diameter and length of this construct will be determined depending on the seeding density of the cells onto the final construct and cell viability after the ends are sealed off using heat shrink.

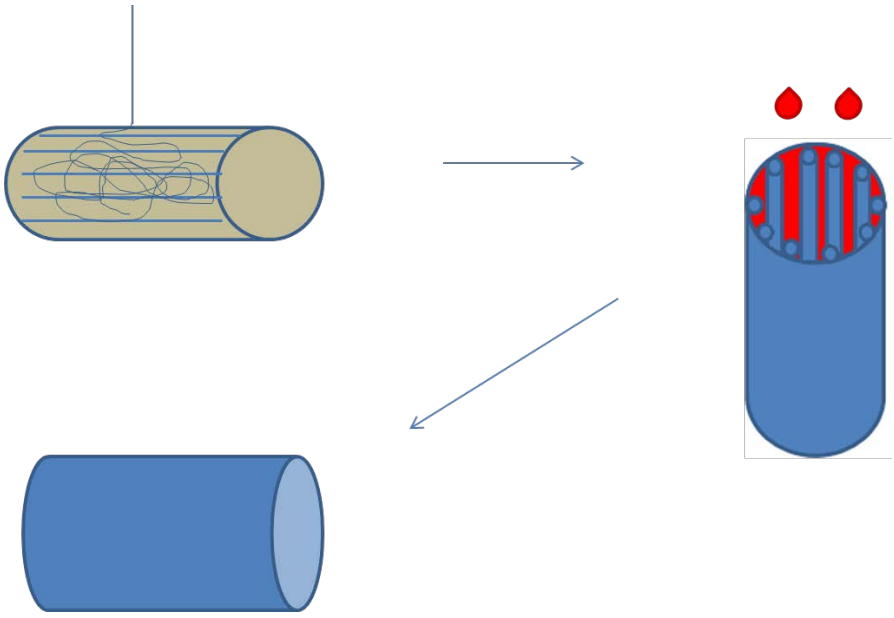

Figure 4.9: Design Alternative 1

Alternative design 2 is a modification of the preliminary design 5, which is a rectangular shaped scaffold allowing for higher seeding density as compared to that on a cylindrical construct. This seeding density data has been obtained from the Myocardial Regeneration Lab at WPI. But instead of starting with a flat sheet, this rectangular scaffold construct will be obtained from the fibrin supported cylindrical construct as described in the alternative design 1. Once the large diameter cylindrical scaffold is removed from the mandrel along with its fibrin support structure, the scaffold will be cut open into a flat sheet. Cell seeding will be performed on this flat fibrin-reinforced scaffold, since higher seeding densities have been reported on flat sheets as compared to cylindrical constructs. After the cells are seeded on the upper side of this scaffold sheet, it will be folded over like a sandwich with the seeded cells on the inner side. Finally, the three open ends of this folded construct will be sealed using a custom heat shrink method. The modification made to the preliminary design 5 in terms of using a meshed fibrin support structure instead of parallel rods, will provide better structural and mechanical integrity. Also, we propose to obtain the flat sheet from a cylindrical construct since it was suggested that electrospinning on a cylindrical mandrel results in more uniform porous structure of the scaffold. Just as with the alternative design 1, the

exact dimensions of the resulting final scaffold sheet will be determined depending on the cell viability after the ends of the sheet are sealed off using heat shrink.

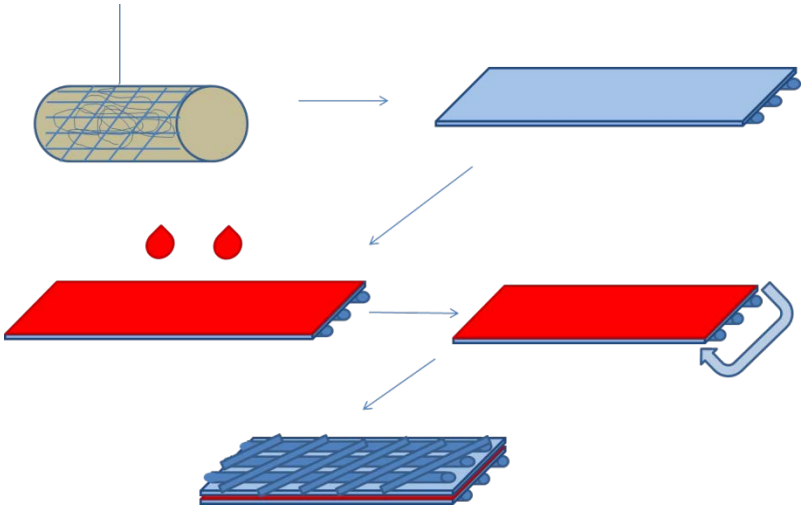

Figure 4.10: Alternative Design 2

4.4 Feasibility Study

With manufacturability being one of the most important functions of the design, extensive feasibility study needs to be performed to mimic different steps of the manufacturing process and to test material properties of the device. When compared with designs from previous years, the major advancement of our designs is the incorporation of fibrin microthreads as supporting structure for the delicate cardiac scaffold. In order to ensure the feasibility of incorporating new elements to existing electrospinning protocol, simple experiments would be conducted using fibrin threads to test for their dissolution property and ease of preparation for electrospinning. In addition, since head shrink would be used to seal the edges of the device, it is crucial to determine the affected area of damaged cells by the heat.

During the initial steps of the electrospinning process, polyurethane would be dissolved to a liquid form using a predetermined solvent. The solvent would then be removed from the electrospun scaffold by soaking the material in two consecutive solvent baths comprised of water and ethanol. Therefore, in order to incorporate fibrin threads to the electrospun scaffold as a supporting material, the fibrin threads must not dissolve in either water or ethanol and retain its mechanical strength after the

liquid baths. A simple dissolution test was performed using dry fibrin threads, which mimic the actual condition of the threads after electrospinning. A strand of fibrin thread was cut into multiple shorter pieces and laid in two separate petri dishes. Either water or ethanol was then added to each petri dish till all pieces of the fibrin threads were fully submerged. Since the electrospun scaffold would be soaked in each solvent bath for 20 minutes in room temperature according to the existing protocol, the threads was also submerged in the solutions for 20 minutes under the same conditions. After the 20 minute period, the threads was removed from the liquids and allowed to be air dried for five minutes. Afterwards, the threads were pulled using tweezers, and the forces required to break the saturated threads were compared with the forces used to break dry threads. The dissolution test showed that the fibrin threads did not dissolve in either water or ethanol, and no significant changes in the mechanical strength of the threads were observed. Therefore, the test validated the feasibility of using fibrin threads as the supporting material for the electrospun scaffold.

After demonstrating the feasibility of incorporating fibrin threads to the electrospinning process, we further tested the ease of preparations required to sufficiently attach and align the threads onto the collecting rod. Ideally, we would want the process to be as flexible as possible by using already made and dried fibrin threads instead of using freshly made threads that have not yet to dry. First, we tried saturating dry threads with water, and then attach them to the rod using water's capillary force. However, saturated fibrin threads proved to be too stiff even after being saturated. This resulted in difficulties wrapping the treads consistently and accurately around the rod, and detachment of the threads from the rod as water evaporates from the surface. As an alternative method, we attempted to use freshly made fibrin threads before they have been dried. After the threads were pulled from the fibrin bath, the wet threads were immediately adhered to a slowly spinning rod in helical and anti-helical directions, which resulted in the formation of a fibrin web covering the surface of the rod. When compared with the dry threads, the wet threads were much more flexible, which resulted in much higher accuracy in maintaining appropriate spacing between the threads, and the threads were able to stay adhered to the rod. In addition, ease of removing the fibrin mesh was also determined. After complete drying of the fibrin mesh on the

collecting rod, the fibrin mesh was saturated in water to allow for some degree of flexibility during the removal. When attempting to remove the mesh, the fibrin mesh was peeled off with only minimal force and there was no chemical bonding between the fibrin mesh and the collecting rod.

Head shrink was proposed to be used as a method of sealing the exposed edges of the folded scaffold to prevent cell migration. The method was chosen to be the preferred sealing method because of the theoretical ease of controlling the scaffold size by modifying the size of heat press. However, extremely high temperature is required to fuse electrospun polyurethane, and the high temperature used has detrimental effect on the viability of the cells. Therefore, to compensate for the reduced cell count within the scaffold, the area and number of cells affected by the heat shrink of the scaffold edges must be determined. To perform the study, hMSCs would be seeded onto one side of the electrospun scaffold and cultured for seven days to allow for cell attachment. Then the scaffold would be folded inward, sandwiching the cells in the middle before the heat shrink. A custom made heat press with the predetermined dimensions would be used to seal the three exposed edges of the scaffold. Afterwards, the sealed scaffold would then be fixed and sectioned. The sections would be stained with live/dead staining and observed under the microscope for affected area and damaged cells. By knowing the affected area and number of damaged cells, we can compensate by increasing the surface area of the scaffold.

4.5 Decisions on Final Design

In choosing between the alternative designs, two major factors were considered to determine the best candidate. Seeding densities for cylindrical and flat polyurethane scaffolds were previously determined in research done by Nancy Duffy. For a tubular construct 2 cm in length and 1 mm in diameter, a cell count of 1100 cells could be achieved. Because of the resulting low seeding density in tubular designs and considering the need for approximately 150,000 cells, it is unrealistic to pursue this design. For a flat polyurethane sheet design, approximately 1200 cells could be seeded per mm^2, making the desired cell count feasible with a design that is 1.5 mm x 10 cm in area when unfolded. When folded

for delivery, the total exposed area still meets the minimum requirement for surfaces enabling cell to cell contact.

Additionally, the deliverability of the two designs had significant effect on the final decision. It was determined that, if feasible, a catheter-based delivery method is highly advantageous compared to a suture-based method. Using a previously designed catheter as a model, it was determined that the inner catheter diameter would require an outer cylindrical scaffold diameter too small to produce the desired cell numbers. However, for a flat sheet design, it was determined that even when folded over itself, the sheet could still be made to fit inside the 1 mm inner diameter of the scaffold while still meeting the required exposed area and seeding density.

Chapter 5 Methods and Results

5.1 Determination of the Scaffold Surface Area

Before fabricating the design of our scaffold, it was imperative to determine the minimum surface area needed to encapsulate the required number of cells for effective pacing of a human heart, while allowing for implantation through a minimally invasive procedure. Using the transfection efficiency of about 60% for HMSCs as obtained from literature (citation), a retention rate of 10% and a safety factor of 2, it was determined that around 150,000 cells would be required for efficient pacing out of the total 1,000,000 injected cells. Also, using the seeding density of 1254 cells/mm^2 on a flat sheet scaffold as determined previously (citation), the minimum scaffold surface area was calculated to be 1.2cm^2. This area translated into a scaffold sheet with dimensions 40mmx 1.5mm for easy implantation through a catheter.

5.2 Mandrel

Using a schematic supplied by Saif Pathan, Biosurfaces Inc., two mandrels were constructed. These were used as a base to electrospin the desired scaffolds. Each mandrel is made from stainless steel with a length of 30.48 centimeters (1 foot) and a diameter of about 3 centimeters (1.25 inches). Figure 5.1 shows both mandrels fully assembled.

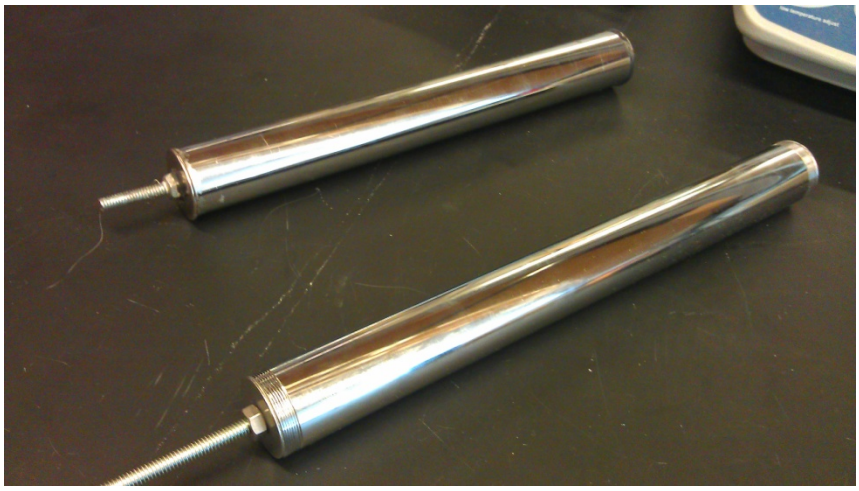

Figure 5.1: Constructed mandrels based on Biosurfaces schematic

The spin time used to create the scaffold is a major contributor to thickness and pore size. At a spin time of 30 minutes, the scaffold proved to be too thick. While the pore size passed the migration test, a thinner scaffold is most desirable in order to maximize the cell to cell interactions without losing the strength. Once this was determined, a spin time of 15 minutes was tested. Figure 5.2 below shows the control scaffold with a 15 minute spin time.

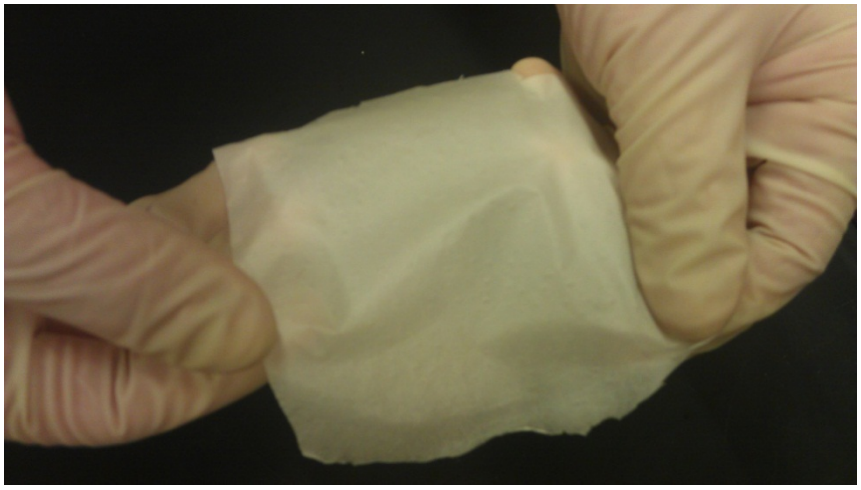

Figure 5.2: 30 minute control scaffold

Fibrin threads were placed on the mandrel to increase the strength of the material as structural integrity tends to decrease with shorter spin times. Figure 5.3 shows a mandrel wrapped with fibrin threads.

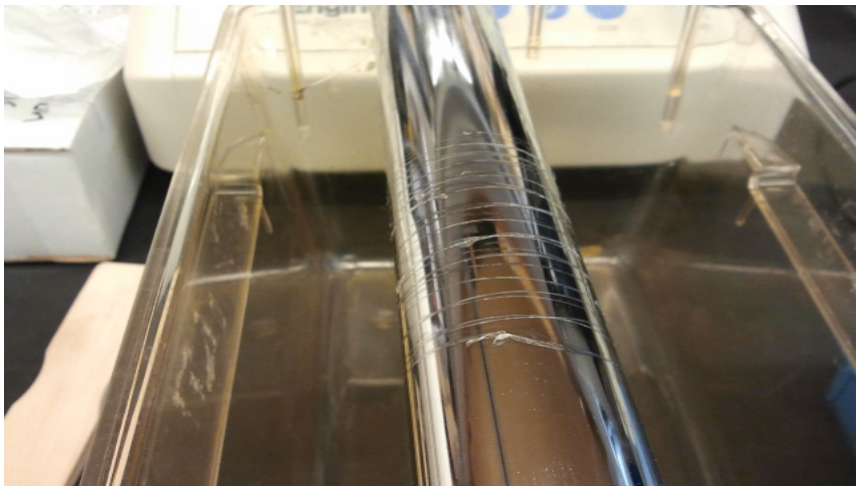

Figure 5.3: Fibrin threads on bare mandrel

Anticipating that the threads would not be easily removed from the mandrels, Teflon tape was wrapped around one of the mandrels. It was speculated that Teflon tape would reduce the fibrin threads adherence to the mandrel making removal of the scaffold with fibrin threads easier. Figure 5.4 below shows a Teflon tape wrapped mandrel with fibrin wrapped around the surface.

Figure 5.4: Fibrin threads on Teflon coated mandrel

After the material was made and removed from the mandrels, it was noted that the fibrin did not adhere to the scaffold in either mandrel. Additionally, it was observed that the fibrin threads seemed to damage the material as it was being removed from the mandrel. So, the fibrin

which was supposed to help strengthen the scaffold actually made it weaker. Figure 5.5 below shows the resulting scaffold from the plain mandrel with fibrin wrapped around it.

Figure 5.5: Scaffold from fibrin coated bare mandrel

Also, the Teflon coated mandrel produced a scaffold that was thicker in some regions than others. This resulted in a spotted pattern. Figure 5.6 shows the resulting scaffold from the Teflon wrapped mandrel with fibrin attached to the surface.

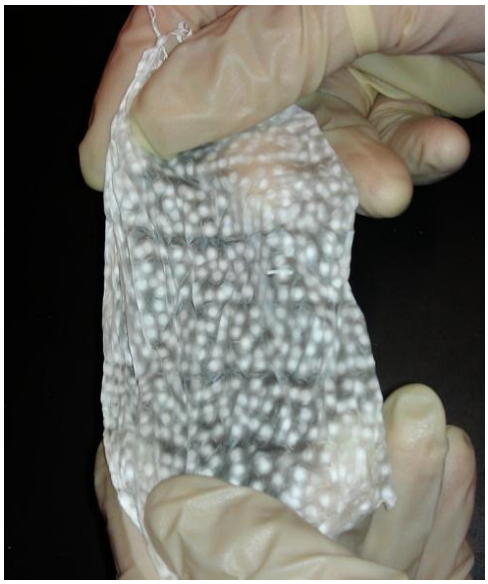

Figure 5.6: Scaffold from Teflon coated fibrin mandrel

However, this setback proved to be a breakthrough in terms of strength. If the spotted regions could be manipulated so that the scaffold displayed patterns of thinner and thicker material, then the strength and thickness problem could be solved. To test this theory, four distinct patterns of Teflon tape were made on the two mandrels. The first pattern completely covered the mandrel leaving no stainless steel visible. The second pattern on the same mandrel formed a spiral that lead from about half way down the mandrel to the end. In this pattern, the Teflon was manipulated so that a thin layer of stainless steel was visible in a spiral pattern. The first pattern on the second mandrel formed stripes along the length of the mandrel. Like the second pattern on the first mandrel, a thin layer of stainless steel was visible. The second pattern on the second mandrel formed a helical structure that consisted of four pieces of Teflon tape. This pattern left a much larger amount of stainless steel visible. Figure 5.7 shows both mandrels with all four designs made out of Teflon tape.

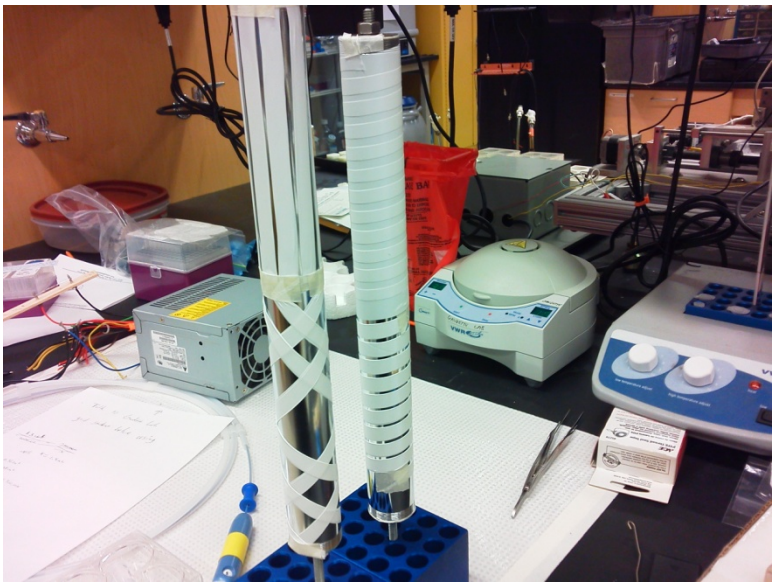

Figure 5.7: Teflon designs on mandrels

The completely covered region reproduced the spotted pattern from the first spin with Teflon. Figure 5.8 below shows the resulting scaffold from this pattern.

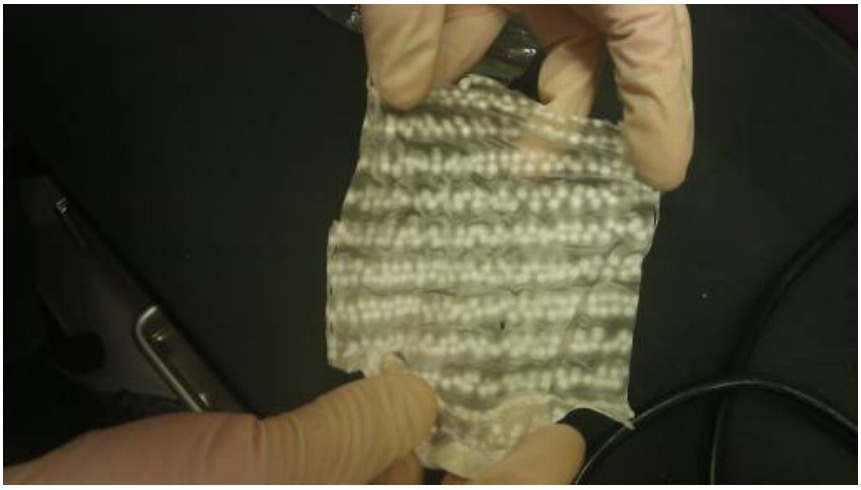

Figure 5.8: Scaffold from completely coated Teflon mandrel

The spiral patterned Teflon region produced a scaffold with evenly distributed regions of thicker and thinner material. Figure 5.9 shows the resulting scaffold from this pattern.

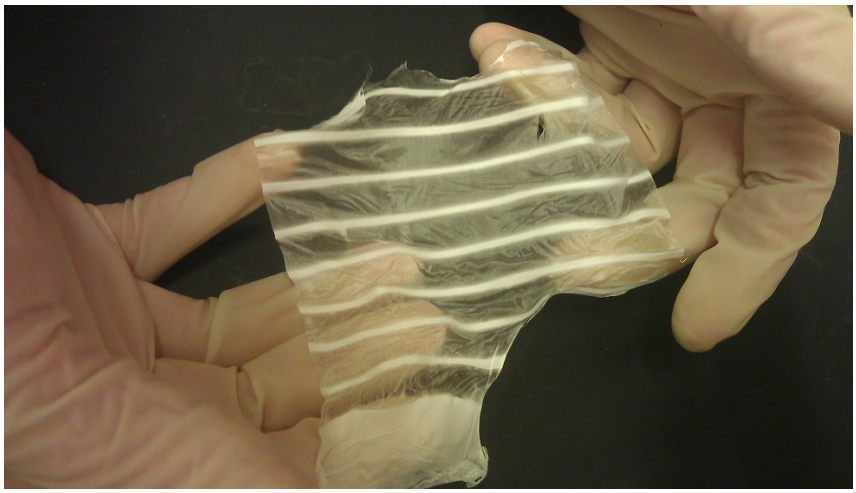

Figure 5.9: Scaffold from spiral Teflon design

The striped patterned Teflon region also produced a scaffold with distributed regions of thicker and thinner material, but the regions were not as evenly distributed. Figure 5.10 below shows the resulting scaffold from this pattern.

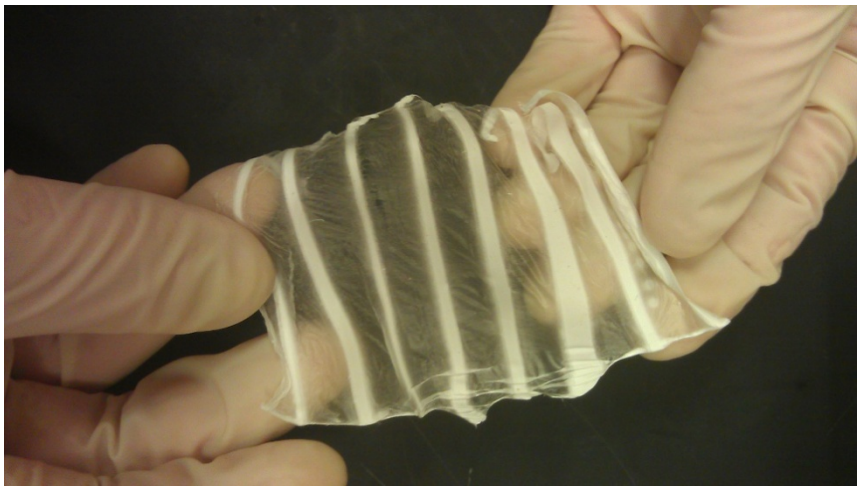

Figure 5.10: Scaffold from stripe Teflon design

The helical patterned Teflon region produced a scaffold with more square regions of thicker material with thinner crossed lines. Figure 5.11 shows the resulting scaffold from this pattern.

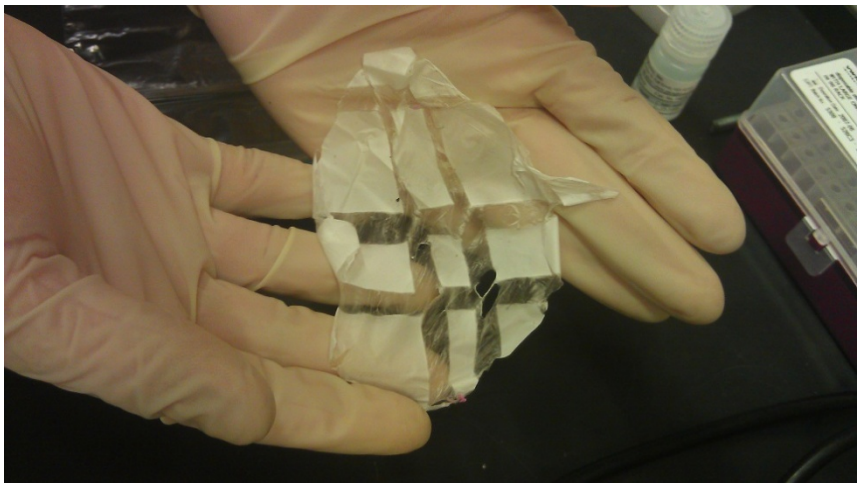

Figure 5.11: Scaffold from helical Teflon design

5.3 Patterned Scaffold Fabrication

Coating the mandrel with Teflon tape resulted in the formation of a patterned scaffold with thick and thin regions, but it was difficult to adhere the Teflon tape onto the mandrel to form intricate patterns. An intricate square pattern (1.5mmx1.5mm) was laser cut onto an adhesive polyester sheet using a Universal Laser Systems VLS4.60 with a 10.6 µm CO_2 laser attachment. The patterned sheet was adhered to a bare metal mandrel and acrylic lacquer was spread on the grooved surface. Excess lacquer was removed and the adhesive sheet was removed after 5 minutes of curing. The lacquer was cured overnight leaving a permanent pattern on the mandrel. BioSurfaces, Inc. electrospun a polyurethane and polyethylene terapthalate blended solution over the mandrel for 30 minutes. The patterned scaffold was obtained after washing in water and ethanol. The obtained electrospun scaffold in this case was intricate with desired thick and thin regions as can be seen in Figure 5.12, but the paint tended to stick onto the scaffold itself while removal.

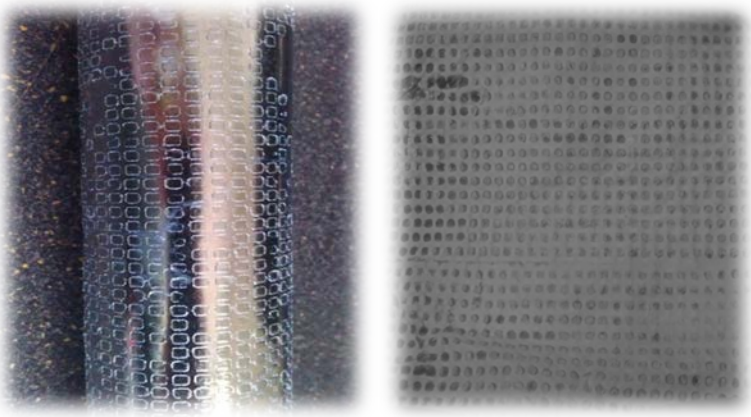

Figure 5.12: Acrylic patterned mandrel (left) and 30 minute electrospun sheet produced by acrylic patterned mandrel (right)

Next, an epoxy material was used to coat the mandrel with the intricately patterned transparency sheet. Following the same procedure as with acrylic lacquer, the adhesive sheet was removed and the epoxy was left to cure overnight to produce a pattern on the mandrel as seen in Figure 5.13 below. The PU/PET blended solution was then electrospun on the mandrel for 60 minutes. The use of epoxy eliminated the problem of the paint sticking onto the scaffold, but the difference in the width of the thin and thick regions of the resulting scaffold was reduced as can be seen in Figure 5.13.

Figure 5.13: Epoxy patterned mandrel (left) and 60 minute electrospun sheet produced by epoxy patterned mandrel (right)

5.4 Migration Testing

With the electrospun blend of PU/PET, it was imperative to determine the average pore size in the resulting scaffold. This was essential because one of the main functions of the scaffold is to prevent the migration of HMSCs from the implant site to the other areas of the heart. The average diameter of

HMSCs is about 10µm and they can also deform under physiological conditions. Taking these two factors into consideration, it was deemed appropriate that the scaffold, spun at 15mins spin time with a thickness of approximately15µm, should have an average pore size of less than 5µm.

The pore size of the scaffold was determined by conducting migration testing using colored microspheres of 5µm diameter. A section of the scaffold (1.7mm x 1.4mm) was cut and placed on the mesh of a Gaudette- Pins well. Once tightly secured within the well, the entire well was placed in a petri dish. For the first round of testing, the microspheres solution with a starting concentration of $1.3x10^8$/ml was diluted 100-fold in deionized water. This dilution factor was calculated by determining the average number of cells that would be present on that size of scaffold section, taking into account the average number of cells (~200,000) to be held in our final scaffold design and the seeding density of cells onto the scaffold (~1200 cells/mm^2), 200µl of diluted microsphere solution was then poured into the Gaudette-Pins well with the secured scaffold section and allowed to sit for 15 minutes shown in Figure 5.14.

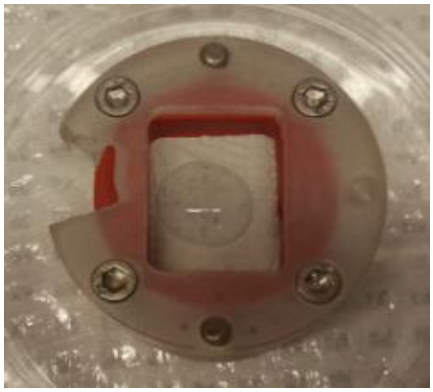

Figure 5.14: Scaffold section clamped in a Gaudette-Pins well with the microsphere solution at 100-fold dilution poured on the top side

The scaffold section was retrieved from the well, carefully placed on a slide, and covered with a coverslip. This section with the microspheres side on the top was viewed under the microscope. Later, the scaffold section was flipped upside down and viewed under the microscope. It was observed that a comparatively larger number of microspheres were visible on the top side of the scaffold where the microsphere solution was poured in comparison to the bottom side. However, the microspheres were hard to identify and could not be visualized under the microscope. Still, in certain areas of the scaffold there

were tears. Here, the microspheres could be seen more clearly. In those areas, more microspheres seemed to have migrated from the top to the bottom side of the scaffold.

For better visualization of the microspheres' migration, this experiment was repeated with a more uniform section of the scaffold and a dilution factor of 1/2 for the microspheres solution. Also, a higher volume (400µl) of diluted solution was poured onto the middle of the secured scaffold section in the Gaudette-Pins well. The higher volume was used so as to be able to test the supernatant for the presence of microspheres. The green color of the solution was clearly visible at this concentration showed in Figure 5.15 below.

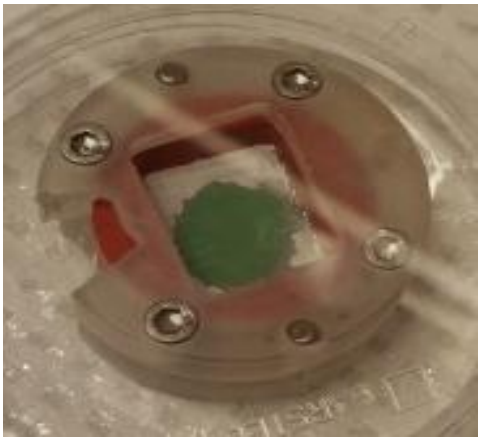

Figure 5.15: Scaffold section clamped in a Gaudette-Pins well with the microsphere solution at 1/2 dilution poured on the top side

When viewed under the microscope after 15 minutes, a very large number of green circular discs were clearly seen on the top side of the scaffold shown in Figure 5.16 below. The density of microspheres on this side of the scaffold was so high that the individual fibers of the scaffold could not be seen. In contrast, the bottom side showed the presence of nearly no microspheres with a slight shadow indicating microspheres on the other side of the scaffold and shown in Figure 5.17. The supernatant left behind in the petri dish was also seen under the inverted microscope for the presence of microspheres. No microspheres were visible in the supernatant shown in Figure 5.18.

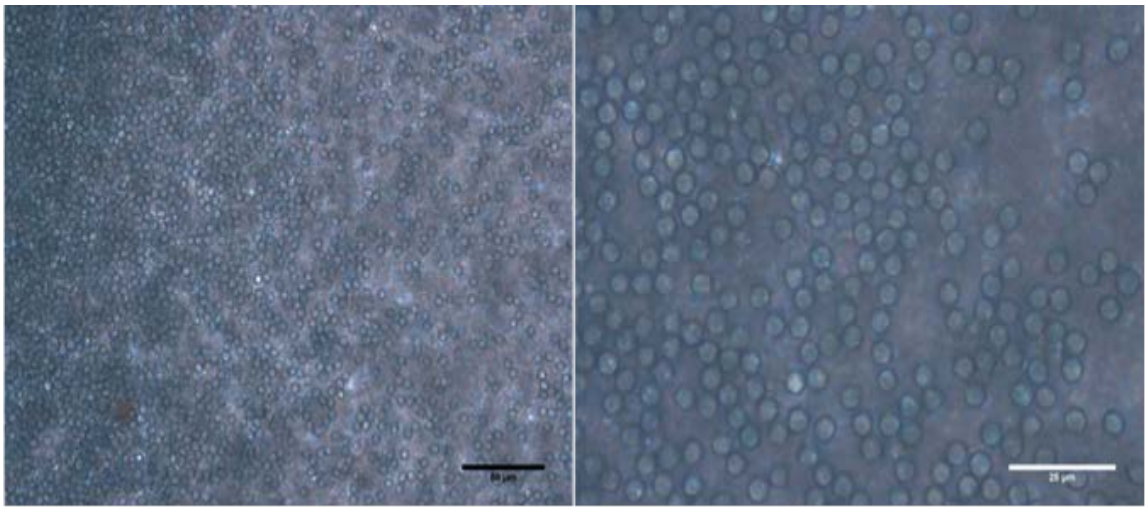

Figure 5.16: Top view of the scaffold section with microspheres (left) taken at 40x and (right) taken at 100x oil bar = 25µm

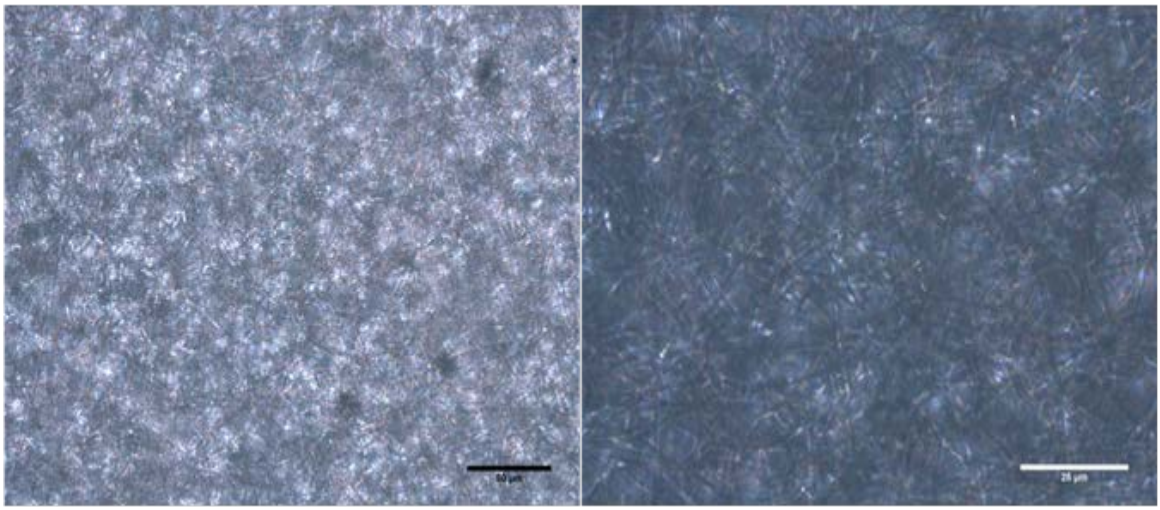

Figure 5.17: Bottom view of the scaffold section (left) taken at 40x (right) taken at 100x oil, bar =25µm

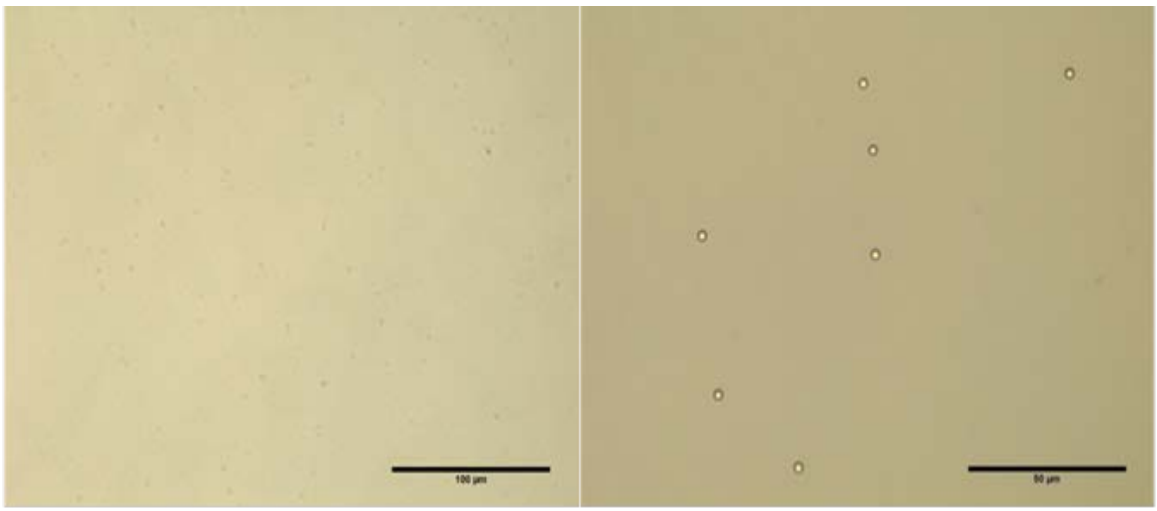

Figure 5.18: Supernatant showing the presence of no microspheres taken at 20x (left), Microspheres on a glass slide taken at 40x (right), bar=25µm

Further migration testing with microspheres was performed on the new scaffold designs incorporating the thick and thin regions of the material obtained by Teflon coated mandrel. A section of the patterned scaffold was secured in a Gaudette-Pins migration well and a mixture of microspheres and DI water in 1:1 ratio was pipetted onto the scaffold. Once the subnatant fluid was accumulated below the migration well, it was imaged alongside the top and bottom surfaces of the scaffold for the presence of the microspheres. The subnatant from the patterned scaffold spun at 15 mins as seen in the Figure 5.19A shows the presence of microspheres. This was due to imperfections in the scaffold as seen in the Figure 5.19B with large pores between the scaffold fibers. Thus, the teflon coated scaffold spun at 15 mins failed to prevent microsphere migration.

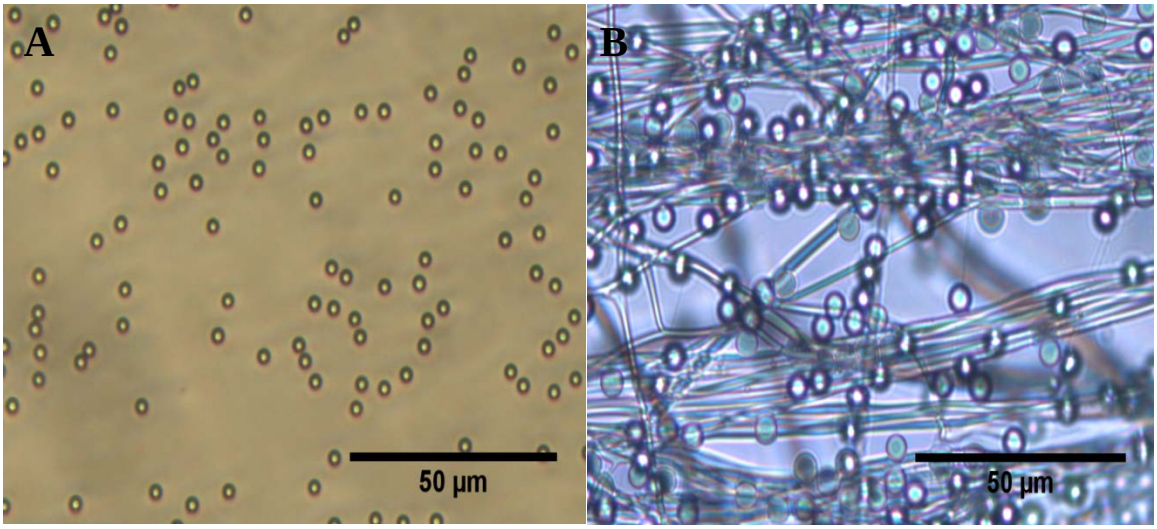

Figure 5.19: Subnatant from a 15 min teflon patterned scaffold showing the presence of microspheres taken at 20x (left, Figure A), Teflon patterned scaffold spun at 15 min showing imperfections (right, Figure B)

The same migration testing was performed on the patterned scaffold obtained after 30 mins of electrospinning on the acrylic-coated mandrel and produced similar results as seen in Figure 5.20.

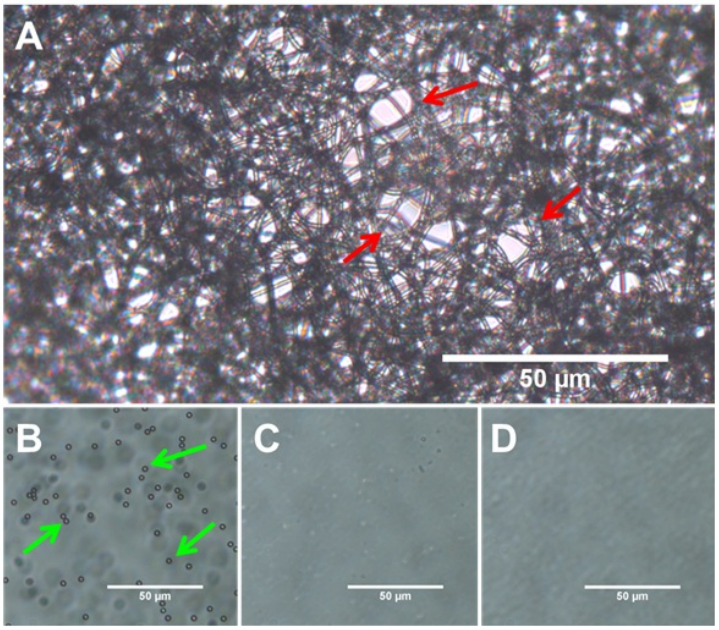

Figure 5.20: A) 30 min acrylic patterned scaffold with imperfections in the thin regions shown by the arrows [red]. B) Positive control of subnatant with arrows [green] pointing to microspheres. C) Negative control with DI water only. D) Subnatant of 15 min flat scaffold showing no microspheres.

Finally, migration testing was performed on an epoxy patterned scaffold spun at 60 minutes. It can be clearly seen in Figure 5.21 below that the subnatant from the sample scaffold showed no presence of microspheres. So, the 60 min epoxy patterned scaffold was successful in preventing microsphere migration.

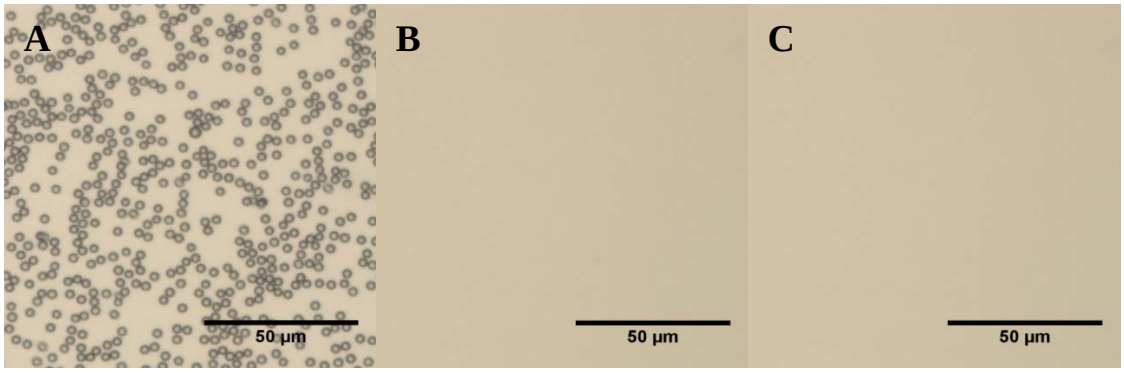

Figure 5.21: Positive control with microspheres (left, Figure A), Negative control with DI water (middle, Figure B), Subnatant of 60 min epoxy patterned scaffold showing no microspheres (right, Figure C)

5.5 Heat Sealing

Once it was determined that heat sealing would be the best method for bonding the edges of the scaffold to each other, a functional heating element had to be created. The initial design of a heating element, shown in Figure 5.22, consisted of a 9 volt battery with positive and negative leads running to opposite ends of a copper wire mounted between two finishing screws. Power was regulated with an on/off switch.

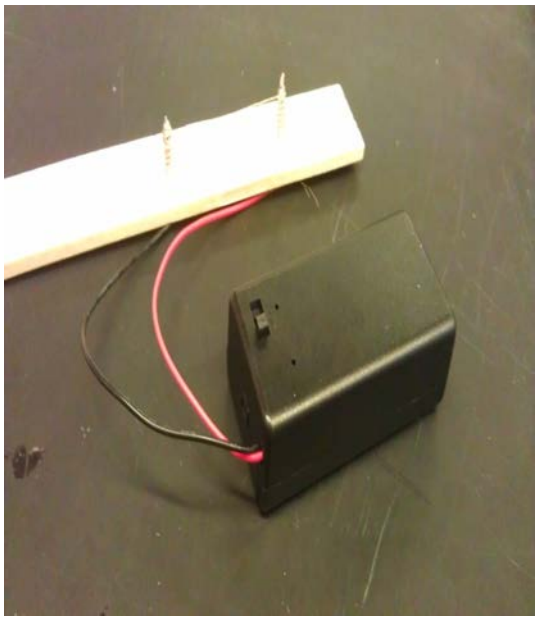

Figure 5.22: Preliminary heating element

Testing of the first device was done with folded 50 μm thick pieces of scaffold. Power was turned on and the unit was tested at standard time intervals. Initial testing was conducted to determine if the heating element could melt the scaffold at each time point. Data from this experiment is shown in Table 5.1 below.

Table 5.1: Time connected to the battery

Time On (s)	Melting (Y/N)
5	N
10	N
30	N
60	N
120	N
180	N

A second heating element, shown in Figure 5.23, was designed using a 12 volt 18 amp computer power supply unit (PSU). This unit consists of positive and negative leads each of which is connected to an end of a steel wire 4.5 cm in length. Because PSU's are designed with a switch that prevents the supply from running after a short circuit, an additional switch was added to circumvent this failsafe.

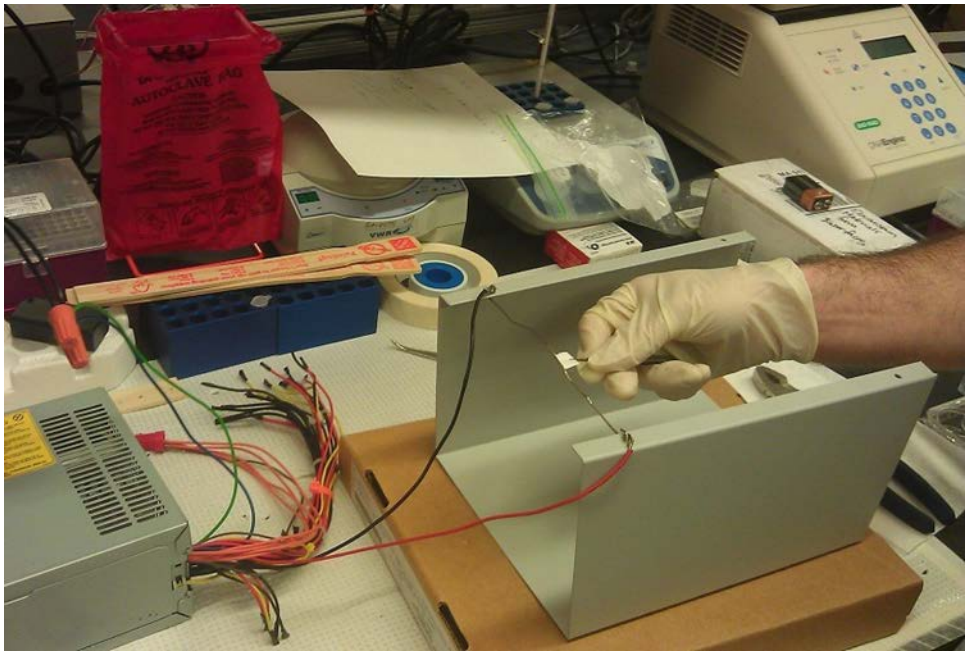

Figure 5.23: Second iteration heating element

Because this second design did not have a continuous flow of power, the same initial test was conducted using "number of clicks" of the power switch as the independent variable instead of time. Once again, testing was done first to see if melting was possible. This experiment was done with 50 µm folded scaffold pieces. The data from this experiment is shown in Table 5.2 below.

Table 5.2: Number of clicks relative to scaffold sealing

# of Clicks	Melting (Y/N)
1	N
2	N
3	Y
4	Y
5	Y

A third iteration of the heating element was designed so that a scaffold could be brought near the heated surface gradually to avoid catastrophic failure of the polymer mesh by overheating. This design used the same PSU and positive and negative leads. Because a wire complicated sealing of the edge of scaffold which is less than 50 µm thick, it was replaced with a 1”x8” copper ribbon. This ribbon would allow the edge of the scaffold to be pressed against the heater to make sealing easier and more precise. Folded 15 µm samples were tested at different intervals of distance and time to optimize distance from the heating element and time under heat.

A final iteration of the device was made using a power supply provided by Worcester Polytechnic Institute. The new power supply allows for controllability of voltage and current going into the resistance heater. This allows for variation in temperature, allowing for optimization of temperature to be determined. The final design, shown in Figure 5.24 below, consists of two acrylic bases connected by steel rods. A 4” strip of copper tape is connected to the end of the rods by polymer weld.

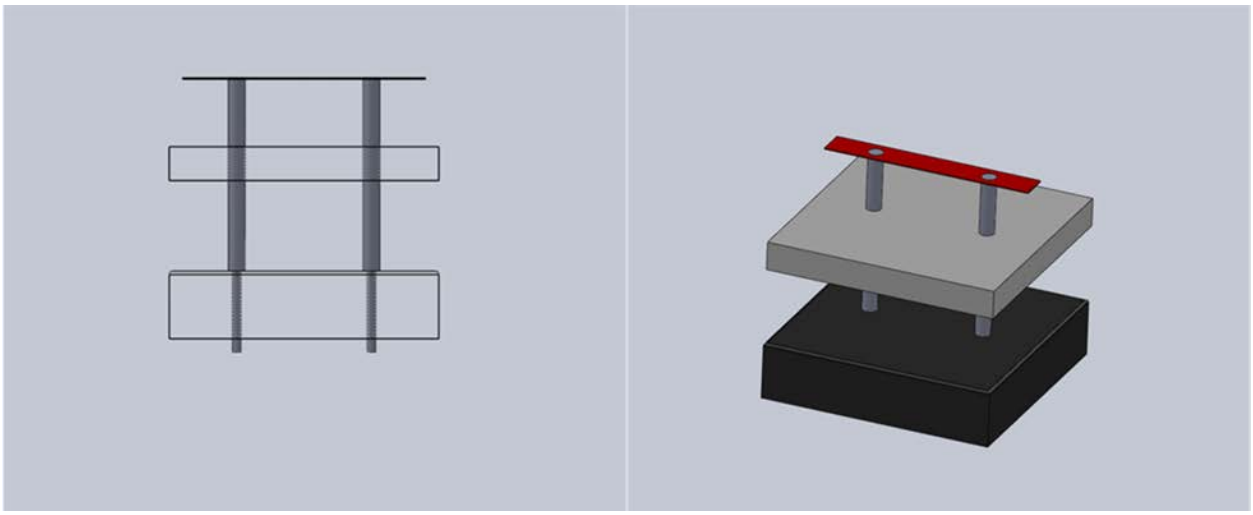

Figure 5.24: Final base design for heating element

An alternative design was drafted with the intention of having a heat press which could simultaneously heat and seal 4 edges of the device while cutting out the shape of the scaffold. However, this design was deemed too difficult to manufacture with the resources available in the WPI machine shop within the time constraint of the project.

To systematically test the effect of distance from heating source and temperature of the heating element on the sealing of the scaffold, a slider mechanism was designed and implemented in testing. A retractable metal slider was mounted on a fixed platform with scale marking in millimeters. To this slider, a modular chuck was mounted that clamped the scaffold into place. The chuck was moved incrementally to determine the proper distance for heating the scaffold edges while minimizing cell death. Time intervals of 1, 2, 3, 4, and 5 seconds were also measured at each distance increment to optimize time at a given distance. As shown in Figure 5.25 below, the modular chuck has three open sides to expose the open edges of the scaffold for heat sealing.

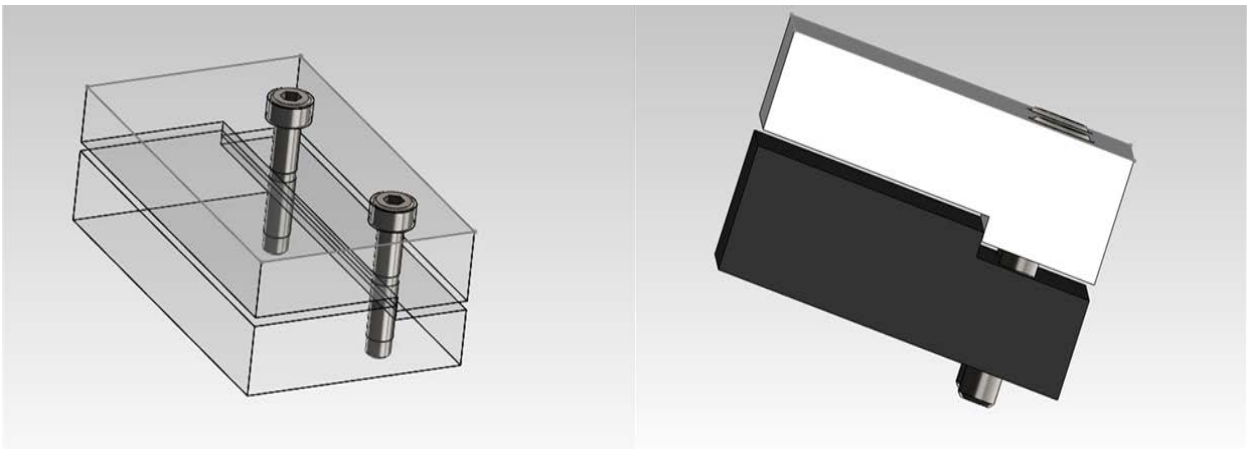

Figure 5.25: Modular chuck for clamping the scaffold

5.6 Fabrication of Sealed Scaffold

To produce a sealed scaffold for cell implantation, the electrospun scaffold was folded and heat sealed using the final iteration of the heating device. Using the components of this device as shown in Figure 5.26 below, the folded scaffold was secured in a custom made PDMS clamp attached onto a manually controlled slider, which was used to move the secured scaffold towards the heating element. The scaffold was briefly touched to a heating element consisting of a copper wire raised to approximately 155^{o}F. This mechanism allowed for the complete sealing of the edges.

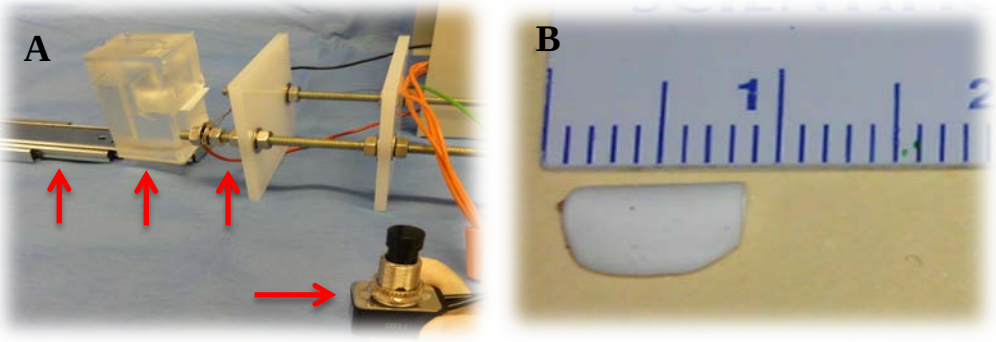

Figure 5.26: Sealing the folded scaffold using a heat sealing mechanism consisting of a slider, clamp, heating element and a power switch as shown by the red arrows (left, Figure A), Sealed scaffold (right, Figure B)

To verify that the edges of the scaffold were completely sealed, migration testing was conducted using the sealed scaffold seeded with microspheres. 5 µL of 1:1 mixture of microspheres and DI water was pipetted onto a section of scaffold, which was then folded and heat sealed after drying. The sealed

scaffold was placed in a microcentrifuge tube with 500 µL of DI water and agitated for 10 seconds with a Daigger Vortex Genie 2 vortexer. The surrounding liquid was then imaged for the presence of microspheres. No microshperes were observed in the supernatant as shown in the figure below, indicating that the edges of the folded scaffold were completely sealed by heat.

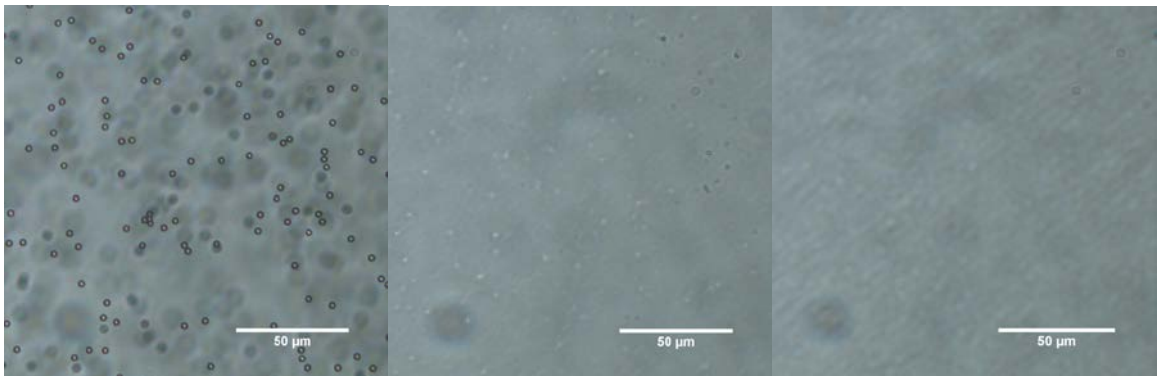

Figure 5.27: Positive control with microspheres (left), Negative control with DI water (middle), Sample supernatant showing no microspheres (right)

5.7 Implant Testing

To ensure that the device can withstand the forces involved in the heart contractions and implant forces, a small piece of scaffold was loaded onto a catheter. Figure 5.28 shows the size of the scaffold used for implant testing, and the second figure shows the piece of scaffold loaded onto the catheter.

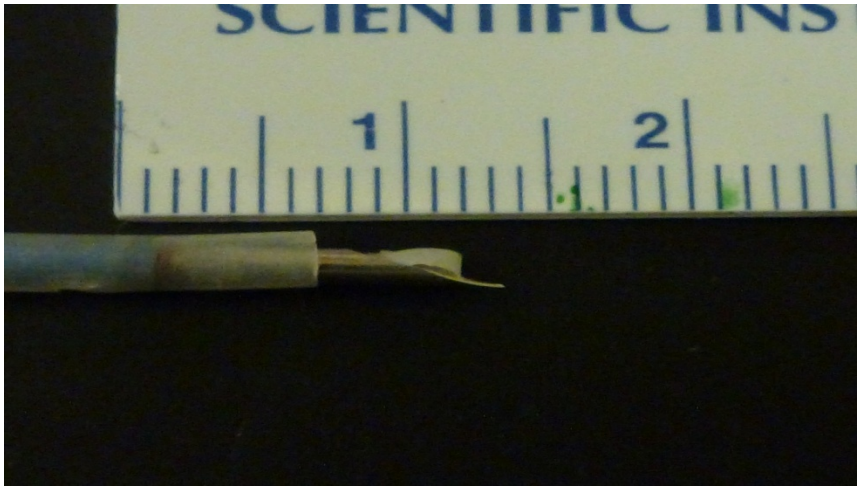

Figure 5.28: Scaffold loaded in catheter

Then, the loaded catheter was forced through a rat heart and pulled back out. It was noted that there was still a piece of the scaffold on the end of the catheter. The figure below shows the loaded catheter going into the rat heart.

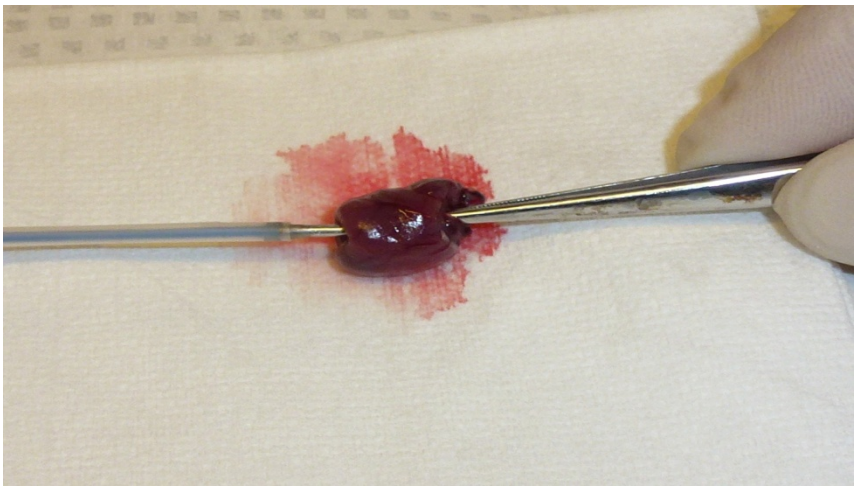

Figure 5.29: Insertion of catheter needle into rat heart

It was suspected that the scaffold stuck because it was not properly hydrated. So, the test was conducted again with proper hydration and the scaffold was completely off the catheter. Figure 5.30 below shows the rat heart with the scaffold held in place after the catheter was removed.

Figure 5.30: Scaffold embedded in the rat heart

This means that the scaffold stayed in the heart when the catheter was removed, and that it is able to withstand the shear forced associated with implantation forces.

Further implant testing was conducted using an explanted pig heart. A piece of a scaffold was loaded onto the tip of a 4-stage catheter and inserted into the ventricular wall of an explanted pig heart through a makeshift aorta. The needle of the catheter was first pushed through the heart wall and then the inner core of the catheter with the loaded scaffold piece was extended out. Finally, both the inner core and the needle were retracted and pulled out of the makeshift aorta, leaving behind the scaffold piece in the heart wall as seen in the figure A below. The scaffold piece was later retrieved and was visually inspected for any tears or failure. After the scaffold was extracted from the heart, it was observed that there were no tears or deformations. Though the scaffold piece appeared to fold on itself due to wetting, it did maintain its structural integrity during implantation, as seen in figures B & C below.

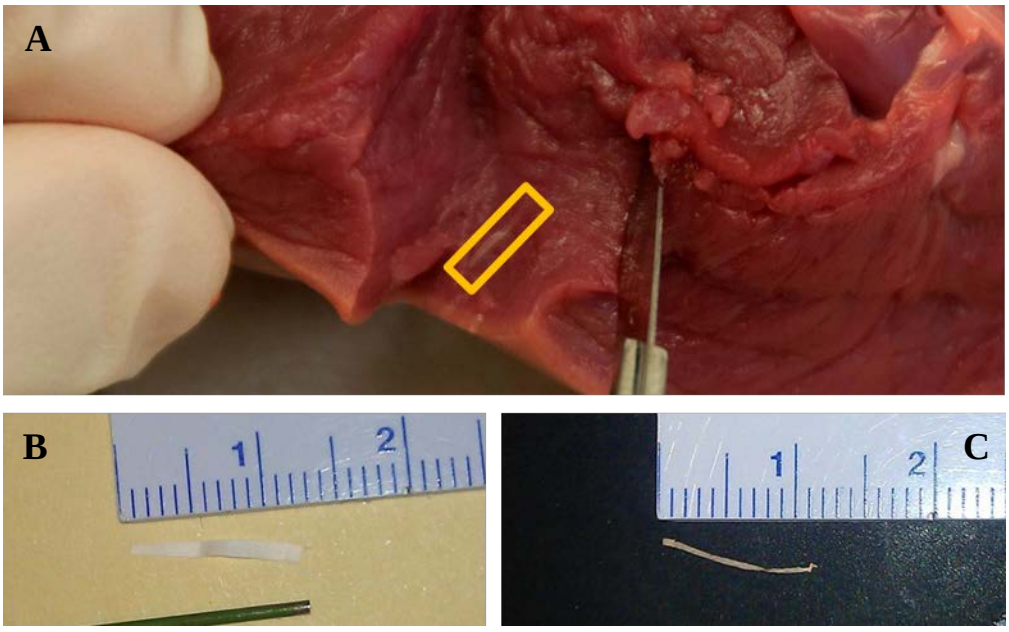

Figure 5.31: Implanted scaffold in an explanted pig heart (top, Figure A), Scaffold before implantation (left, Figure B), Scaffold after implantation (right, Figure C)

Chapter 6 Discussion

An effective minimum scaffold surface area to encapsulate the required number of cells was determined using the data from previous research. This size took into consideration that all the cells encapsulated within the scaffold need not be in direct contact with the native cardiomyocytes, since the signal would be passed along the cells. The loading of the scaffold sheet with the current dimensions, onto the tip of a catheter was difficult even after wetting of the scaffold material. In the future, the calculated dimensions of 40mmx1.5mm could be reduced further as the transfection efficiency of the HMSCs is approaching closer to 100%. The resulting smaller size of the scaffold would allow for easier loading onto a catheter device and implantation.

Providing the scaffold with the desired mechanical strength was an important objective to ensure that the scaffold can withstand the shear forces during implantation and performs its function effectively by keeping the cells encapsulated. The initial use of fibrin threads to coat the mandrel failed to impart structural integrity to the electrospun scaffold, since the fibrin threads had greater adherence to the mandrel itself and in some cases even caused the scaffold to tear while removal from the mandrel after electrospinning. This problem was approached by coating the mandrel with Teflon tape, which did allow for comparatively easier removal of the fibrin threads from the mandrel. But, the fibrin threads still did not adhere properly to the scaffold upon removal from the mandrel. This was possibly because of the fibrin threads being washed off during the bath step in ethanol and water after electrospinning.

In another aspect, coating the mandrel with Teflon tape proved advantageous, since it resulted in a patterened scaffold. This occurred because of the low conductivity of the Teflon tape in comparison to the bare steel mandrel. It was known earlier that a thickness of about 10µm is desirable in the scaffold to allow for gap junction formation. However, a greater thickness of about 50µm is needed to ensure mechanical strength of the scaffold. Thus, it was deduced that combining these two thickness regions in the same scaffold would provide the desired characteristics to our scaffold with the thicker regions increasing the structural integrity and the thinner regions allowing for gap junction formation between the

encapsulated cells and the native cardiomyocytes. Considering the small size of our scaffold, it was essential to scale down the pattern on the electrospun scaffold. This was difficult to achieve using the Teflon tape because of its low adherence to the mandrel itself. So, another approach was taken to produce a more stable intricate pattern on the mandrel. A laser cut adhesive transparency sheet produced an intricate pattern, onto which materials like acrylic lacquer or epoxy could be easily sprayed/spread, leaving behind a permanent pattern on the mandrel. This pattern was effectively reversed onto the electrospun scaffold to produce a patterned scaffold. However, both the materials did have some limitations. The acrylic patterned mandrel proved to be the most effective way of fabricating the patterned scaffold with the desired structural integrity and thickness. But, repeated fabrication of similar scaffolds would be difficult in the future since the patterned acrylic loses integrity on the mandrel. While epoxy maintains sufficient integrity on the mandrel, making fabrication repeatable, the difference in thickness between regions is greatly reduced due to the higher conductivity of the epoxy. Thus, a less conductive polymer that is stable in ethanol may produce a scaffold with better properties and reproducibility.

A flat electrospun scaffold with 15 minute spin time showed no microsphere migration and had a thickness of about 10μm desirable for gap junction formation. The thickness of this flat sheet could effectively be increased for mechanical strength by using a higher spin time. But, as mentioned earlier, the higher uniform thickness of the scaffold would hamper the gap junction formation. Thus, migration testing was performed on the patterned scaffolds to ensure that the thin regions would prevent cells from migrating and to determine the appropriate spin time for the formation of patterned scaffolds. It was observed that the patterned scaffold spun at 15 and 30 minutes failed to prevent the microspheres from migrating through the pores. The thinner regions of the 15 and 30 minute patterned scaffold showed microscopic imperfections. The microscopic imperfections observed on the 15 and 30 minute patterned scaffolds could be the cause of microspheres migrating through the material. A patterned scaffold produced via a 60 minute spin on an epoxy patterned mandrel was able to prevent microsphere migration into the subnatant, even though the desired difference in thickness between the square and columnar regions of the scaffold was too low for this application. These results of migration testing on the various

patterned scaffolds were promising since they indicate that once a suitable material is found to coat the mandrel resulting in the desired thick and thin regions, the spin time could be adjusted corresponding to the conductivity of that material to ensure no migration through the thinner regions of the patterned scaffold.

Similarly, the results of the migration testing of the heat sealed scaffold could be extended to a patterned scaffold. Because the 15 minute flat scaffold showed no microspheres in the surrounding fluid once sealed, it confirms the effectiveness of the heat sealing mechanism and it can be inferred that the heat sealed patterned scaffold will yield similar results. Nonetheless, the heat sealing device still has a lot of room for improvement, especially in terms of better control of the temperature to which the heating element is raised. This could be worked upon with the currently devised heat sealing system, by trying different materials for the heating element itself.

After observing no tears or deformations present on the scaffold when it was removed from the heart, it is anticipated that the scaffold can withstand the forces active during implantation. But, since this implant testing was done on an explanted rat and pig heart, it does not indicate whether the scaffold would have sufficient mechanical strength to withstand normal cardiac forces. This could be easily tested by extending this study to implant a piece of scaffold in vivo in a beating rat heart.

Economics

The design of current electronic pacemakers results in revision surgeries approximately every ten years. Each reoperation requires more materials to produce replacement battery packs, leads, and controllers. Compounded with the cost of each surgical procedure, electronic pacemakers can be extremely costly over a lifetime. This device uses a small amount of material for the scaffold, and it can remain in the body indefinitely. Thus, biological pacemakers are incredibly cost-effective when compared to electronic pacemakers.

Environmental Impact

As previously stated, current electronic pacemakers require revision surgeries approximately every ten years. This means that more materials are needed to produce the replacement parts. This device

uses a small amount of material used as a scaffold to hold the cells in place, and the device only needs an initial implantation surgery. This consumes less material and is more environmentally friendly than current electronic pacemakers.

Societal Influence

Improve over the limitations of current metal pacemakers which include electromagnetic interference, limited battery life, lead failure, lack of responsiveness to physical and emotional stress, and the pacemaker cannot grow with pediatric patients. Since the device has no metal components, there will be no electromagnetic interference, no batteries are required, and no leads are used to conduct electrical current. The device will use the body's own pacing mechanism so the device will be able to match the heart's pacing under the stresses accompanied with physical and emotional variances. If the situation is such that a pediatric patient needs this device, then it will be able to continually pace the heart will sufficient impulse for the rest of the child's life.

Political Ramifications

In terms of the global market, this device will greatly shift the market for pacemakers. It is assumed that the market will prefer this device over current metallic models because of its natural properties. Hopefully, by shifting the market in favor of this device, the quality of life for the patients will improve by eliminating the limitations associated with electronic pacemakers.

Ethical Concern

This device is based upon usage of modified stem cells, which are surrounded by ethical concerns due to exploratory use of embryonic stem cells. However, because human mesenchymal stem cells can be harvested from the bone marrow of living adults, there are few ethical issues with their use beyond informed consent of the patient and cell line donor. These issues warrant consideration with normal surgical procedures as well.

Health and Safety Issues

As stated earlier, this device is a great improvement on current metallic pacemakers. Still, there is an issue with containing the cells inside the implanted scaffold. If the pore size of the scaffold is too large

or the edges are not completely sealed, then it is possible that the cells will migrate away from the implantation site. Upon migrating, the cells can settle in other places and cause tumors to form. While containing the cells was a large portion of this project, the procedure for fabricating the scaffold and sealing the edges after seeding the cells is not absolute. As with all surgical procedures, there is the risk of human error. These errors could cause defects in the scaffold which could lead to the cells migrating away from the implant site and decrease the pacing efficiency.

Manufacturability

Manufacturing the patterned scaffold would not be difficult once a patterned mandrel with an ideal material used for coating is made. It can be reused extensively without harming the intricate pattern on the mandrel. This makes removal of the scaffold, after electrospinning on top of the mandrel, very easy as well. The most difficult part of the fabrication would be sealing the device. To ensure a complete seal with full functionality, one must take into account the total shrinkage of the scaffold, cell death upon sealing, and uniform sealing around the scaffold with no imperfections that would allow for the seeded cells to migrate.

Sustainability

The materials used to fabricate this device are readily available and the final product uses a small amount of each. Because only a small amount is used, the risk of depleting these resources through manufacturing this device is almost negligible.

Chapter 7 Final Design and Validation

Due to the inherent limitations of electronic pacemakers, the clinical need for an effective and reliable replacement is significant. With its success in the pacing of canine models, HCN-transfected hMSCs have shown a promising potential in replacing electronic pacemakers. The implantable biological pacemaker design proposed by the project provides a clinically feasible device that can maintain pacing function of the transfected hMSCs by preventing cell migration, in addition to being manufacturable and implantable.

Previous projects have demonstrated that the electrospun scaffold used to fabricate the biological pacemaker is capable of providing sufficient cell viability. In addition, the electrospun material has suitable physical properties to be manipulated into various shapes and designs tailored to specific applications. However, the designed proposed previously were not clinically viable due to difficulties in manufacturing and implantation. The use of fibrin glue to seal the edges of the device is difficult to perform accurately and repetitively. To achieve sufficient mechanical support, the electrospun scaffold used was too thick to allow for the formation of gap junctions.

After developing our client statement and going through the design process, the project has four primary objectives. First, the minimal scaffold surface area needs to be determined to allow the biological pacemaker to be as small as possible in size for easy implantation. Second, the electrospun scaffold needs to prevent cell migration to maintain the pacing function of the HCN-transfected hMSCs. Third, the electrospun scaffold needs to provide sufficient mechanical support, so the device can withstand the forces during implantation. Last, by fulfilling all the previous objectives, a clinically feasible biological pacemaker design that can be delivered through a minimally invasive procedure was developed.

To determine the minimal surface area of the biological pacemaker, the minimal number of HCN-transfected hMSCs required to provide sufficient pacing of a human heart should be assessed. Based on the numbers obtained from literature review, it was determined that 150,000 cells are needed to provide

adequate pacing. With the cell seeding density determined by previous research [] on electrospun scaffold, it was calculated that the biological pacemaker needs a minimal surface area of 1.2 cm^2, which translates to a dimension of 40 mm by 1.5 mm for ease of delivery.

To demonstrate electrospun scaffold's ability to prevent cell migration and to determine the minimal spin time for preventing migration, migration testing was conducted on flat sheets of electrospun scaffolds spun at different times. When 5 μm microspheres were pipetted onto one side of the scaffold, it was found that a flat sheet spun at 15 minutes was able to successfully prevent migration while maintaining a thickness of merely approximately 10 μm.

To allow for gap junction formation, an ideal electrospun scaffold would prevent cell migration while having a low thickness. However, the reduction in thickness significantly weakens the mechanical properties of the scaffold. To ensure that the biological pacemaker has sufficient mechanical strength to withstand the stress and strain during implantation, designs of patterned scaffold were proposed to create scaffolds with thin sections for gap junction formation and a thick mesh for mechanical support. Different materials were used to coat the stainless steel mandrel to create an inverted pattern. The different patterned coatings would change the surface conductivity of the metal mandrel, resulting in a difference in the thickness of the deposition of the electrospun polymer. Each material has its unique advantages and disadvantages. The acrylic lacquer coating had low conductivity, and was able to create an intricate patterned scaffold with distinctive thick and thin sections. However, the acrylic lacquer is not chemically stable and adhered to the scaffold upon removal. On the other hand, the epoxy coating stayed adhered to the mandrel. However, epoxy is highly conductive, resulting in less distinctive thick and thin sections. Ideally, a material combining the low conductivity of acrylic lacquer and chemically stable property of epoxy should be used to coat the mandrel.

Since no feasible sealing methods were proposed previously, a new sealing method was created using the thermal properties of the electrospun scaffold. To ensure ease of repetitive fabrication, a custom heat sealing setup was used, which consisted of a heating element, a PDMS clamp holding the scaffold, and a controlled slider securing the clamp. Scaled models of the biological pacemaker were made by

using microspheres. The sealed pouches showed no leakage of the 5 µm microspheres, demonstrating the effectiveness of heating sealing.

To demonstrate that the electrospun scaffold can withstand the forces during implantation via a catheterization device, a piece of the scaffold with a size of 12 mm x 1 mm was implanted into the left ventricular wall of a porcine heart through the aorta. The scaffold was able to be successfully implanted into the tissue while maintaining its structural integrity.

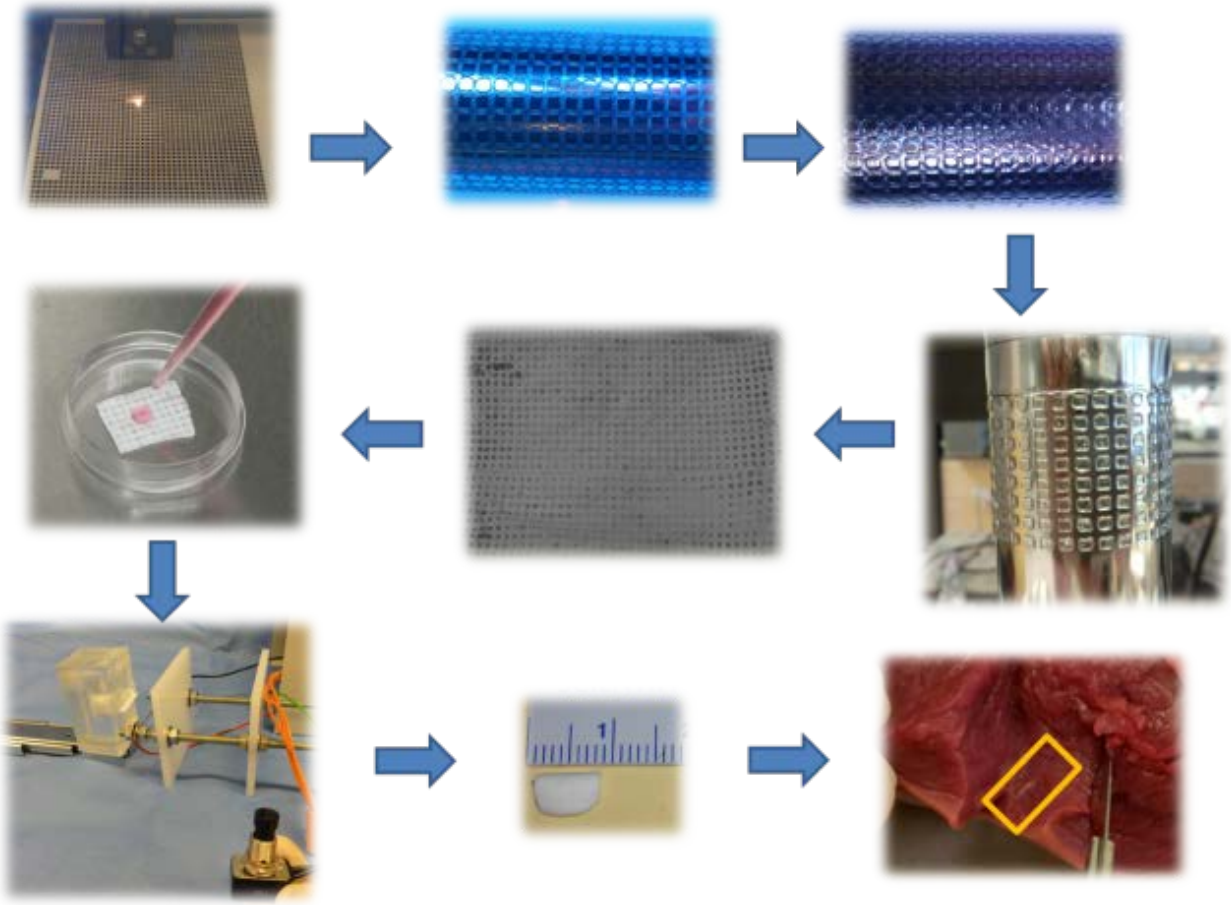

Figure 7.1: Progression of fabrication and implantation of biological pacemaker.

By fulfilling the previous objectives, the team developed a clinically feasible biological pacemaker that can be delivered to the heart using a minimally invasive procedure. As illustrated in Figure 7.1, the fabrication of the device starts with laser cutting of the pattern on an adhesive polyethylene terephthalate sheet. The sheet is then adhered to the stainless steel mandrel to create an

inverted coating. When the PU/PET polymer is spun onto the patterned mandrel, a patterned scaffold with thick and thin sections could be obtained. HCN-transfected hMSCs could then be seeded on one side of the electrospun scaffold. After sufficient cell attachment, the scaffold would then be folded and heat sealed to create a pouch. The pouch fabricated from patterned electrospun scaffold and seeded with the cell could finally be implanted into the heart using a custom catheterization device with an inner diameter that is greater than the width of the biological pacemaker.

Chapter 8 Conclusions and Future Recommendations

Migration testing on flat PU/PET blended electrospun sheets revealed that thicknesses of 10 μm could be achieved while effectively preventing migration. Testing on novel patterned scaffolds demonstrated that thick and thin regions could be established in micropatterns which would provide strength for implantation and allow for gap junction formation between transfected hMSCs and native cardiomyocytes. Models of the final sandwich design were successfully sealed via heat shrinking and retained the microspheres that were sealed inside them when vortexed aggressively in diH_2O. Sample scaffolds were also successfully loaded into a catheter and implanted into the left ventricular wall of an explanted pig heart without losing structural integrity.

Because a suitable polymer for patterning the mandrel before electrospinning was not determined, the first step in continuing research is to find a polymer that is highly insulating, can be spread over the patterned, laser cut stencil, and will adhere to the steel mandrel without solubilizing in water or ethanol during sonication. Once a polymer is determined, an ideal spin time can be determined such that the sheets are <10 μm in the thin regions and >50 μm in the thick regions. Once a proper polymer sheet is developed, cell viability and migration prevention should be reconfirmed. After this is completed, the next recommended step is to confirm gap junction formation using a dye transfer assay. This step will confirm functionality of the device and is essential to moving the device toward clinical application. The final steps necessary to translate this device to the clinic are delivery of models fully loaded with quantum dot loaded cells to explanted hearts via catheter to verify efficacy of the device, and pacing trials in an animal model. It is believed that completion of these future recommendations is necessary to translate this device to clinical applications. In lieu of finding a polymer with the properties described above for coating the mandrel, the research group recommends investigating microfabrication of PDMS membranes using photolithography. This technique would allow for even nanoscale patterns on PDMS membranes of varied thickness.

References

AHA (American Heart Association). "Arrhythmia." 2011.Web.

Anghel, Traian, and Steven Pogwizd. "Creating a Cardiac Pacemaker by Gene Therapy." *Medical and Biological Engineering and Computing* 45.2 (2007): 145-55. Web.

Cohen, Ira S., et al. "The Why, what, how and when of Biological Pacemakers." *Cardiovascular medicine* 2.8 (2005): 374-5. Web.

Costa, Evan, et al. "A Cardiac Catheterization Device for the Delivery of Human Mesenchymal Stem Cells." BS Worcester Polytechnic Institute, 2011. Print.

Cowan, D. B. "A Paradigm Shift in Cardiac Pacing Therapy?" *Circulation (New York, N.Y.)* 114.10 (2006): 986-8. Web.

DiFrancesco, D. "The Role of the Funny Current in Pacemaker Activity." *Circulation research* 106.3 (2010): 434-46. Web.

Freudenberger, Ronald S., et al. "Permanent Pacing is a Risk Factor for the Development of Heart Failure." *The American Journal of Cardiology* 95.5 (2005): 671-4. Web.

Grad, Sibylle, et al. "The use of Biodegradable Polyurethane Scaffolds for Cartilage Tissue Engineering: Potential and Limitations." *Biomaterials* 24.28 (2003): 5163-71. Web.

Institute of Medicine. *A Nationwide Framework for Surveillance of Cardiovascular and Chronic Lung Diseases*. Washington: The National Academic Press, 2011. Print.

Khil, Myung-Seob, et al. "Electrospun Nanofibrous Polyurethane Membraneas Wound Dressing." *Wiley Periodicals* 67B (2003): 675-9. Web.

Mangoni, M. E. "Genesis and Regulation of the Heart Automaticity." *Physiological Reviews* 88.3 (2008): 919-82. Web.

Nancy Duffy. “Characterization of a Fibrin Microthread Biofactory for Delivery of Mesenchymal Stem Cells.” MS Worcester State University, 2011. Print.

Pedicini, Angelo, and Richard Farris. "Mechanical Behavior of Electrospun Polyurethane." *Polymer* 44 (2003): 6857-62. Print.

Potapova, Irina, et al. "Human Mesenchymal Stem Cells as a Gene Delivery System to Create Cardiac Pacemakers." *Circulation research* 94.7 (2004): 952-9. Web.

Qu, Jihong, et al. "Expression and Function of a Biological Pacemaker in Canine Heart." *Circulation* 107.8 (2003): 1106-9. Web.

Rosen, Michael R., et al. "Genes, Stem Cells and Biological Pacemakers." *Cardiovascular research* 64.1 (2004): 12-23. Web.

Rosen, Michael, et al. "Biological Pacemakers Based on I_f." *Medical and Biological Engineering and Computing* 45.2 (2007): 157-66. Web.

Sherwood, Lauralee. *Human Physiology: From Cells to Systems*. 7th ed. Brookes Cole, 2008. Print.

Swan, H. "Mechanical Function of the Heart and its Alteration during Myocardial Ischemia and Infarction. Specific Reference to Coronary Atherosclerosis." *Circulation (New York, N.Y.)* 60.7 (1979): 1587. Web.

Tripathi, Onkar N., Ursula Ravens, and Michael C. Sanguinetti, eds. *Heart Rate and Rhythm: Molecular Basis, Pharmacological Modulation and Clinical Implications.* 1st ed. London: Springer, 2011. Web. Oct.10 2011.

Veronique L. Roger, et al. "Heart Disease and Stroke Statistics--2011 Update: A Report from the American Heart Association." *Circulation* (2010): e18. Web. October 9, 2011.

Wood, M. A. "Cardiac Pacemakers from the Patient's Perspective." *Circulation (New York, N.Y.)* 105.18 (2002): 2136-8. Web.

Appendix A: Viability Testing

In order to determine and demonstrate hMSC viability and attachment on the electrospun scaffold, *in vitro* testing was conducted using a live/dead assay. This assay clearly quantifies the viability of the cells on the scaffold in comparison to the controls on tissue culture polystyrene (TCP).

Thawing and Culturing of Human Mesenchymal Stem Cells

To conduct further *in vitro* experiments evaluating the material properties of the electrospun scaffold, human Mesenchymal Stem Cells (hMSCs) were thawed and cultured. The instructions used to thaw and culture the cells were provided by Jacques Guyette, a PhD alumni, and Mark Kowaleski and Chirantan Kanani, current graduate students in the Biomedical Engineering Department at Worcester Polytechnic Institute.

Human Mesenchymal Stem Cells were used for the in vitro testing because this specific cell type bears the most resemblance with the genetically engineered pacemaker cells, which are hMSCs transfected with HCN genes. Prior to thawing, growth media was prepared in the laminar flow hood by adding 50 mL of fetal bovine serum (FBS) and 5 mL of PenStrep to a bottle of 500 mL DMEM to create a 10% FBS and 1% PenStrep solution. Because the hMSCs were intended to be harvested within a week for live/dead assay and we are not performing any cell treatment, higher passage cells were sufficient for our purpose as long as they still proliferate at a reasonable rate. As preparation for thawing, 5 mL of warmed growth media was added to a 15 mL conical tube and the appropriate vial containing the frozen cells were chosen from a cell inventory sheet. Adequate personal protective equipment was worn when taking the interested vial from the cryotank. As soon as the vial was removed from the cryotank and was slightly warmed to avoid bursting of the frozen vial, the vial was half way immersed in 37 °C water bath till the content of the vial was completely thawed. Since the cryoprotectant containing dimethyl sulfoxide (DMSO) is toxic to cells in liquid form, the cells in cryoprotectant were immediately transferred drop-wise to the 15 mL conical tube containing the growth media. Standard protocol for cell passaging was followed from here. The cell suspension was spun down at 1,000 rpm for 5 minutes in a centrifuge, and

the resulting cell pellet was resuspended in 1 mL of the growth media. Cell counts were achieved by taking 10 μL of the cell suspension and adding it to a small vial containing 10 μL of even mixture of phosphate buffered saline (PBS) and trypan blue dye. After proper mixing of the cell suspension with the dye solution, 10 μL of the mixture was injected into a hemocytometer and counted using an inverted microscope. After calculating the total cell number, the hMSCs were plated in T-75 culture flasks at a seeding concentration of 500,000 cells per flask. For optimal cell proliferation, each T-75 flask was filled with 9 mL of the growth media. The media was exchanged the day after thawing, and every other day afterwards.

The hMSCs were cultured in the T-75 flask for a week till complete confluence. The cells were then harvested using the established protocol. Since FBS in the growth media deactivates trypsin, the media in the flask was aspirated and replaced with 9 mL of PBS to rinse off any remaining FBS. To break down the extracellular matrix that adheres the cells to the surface of the flask, 6 mL of trypin, a serine protease that cleaves peptide bonds within the extracellular matrix, was added after the PBS was aspirated. As an enzyme, trypsin exhibits greatest activity at the physiological temperature of 37 °C. To accelerate the breakdown of the extracellular matrix and to reduce damage to the cells, the flask was placed back into the incubator for 5 minutes. After taken out of the incubator, the flask was checked under the inverted microscope for cell attachment. When no cells were visibly attached to the bottom of the flask when agitated, the trypsin solution containing the cells was transferred to a 15 ml conical tube with 5 mL of growth media. Additional 4 mL of media was used to rinse the T-75 flask to remove any lingering on the plastic surface and again transferred to the conical tube. The content of the conical tube was carefully mixed to ensure full deactivation of the trypsin. Similar to the thawing procedure, the cell suspension was then spun down at 1,000 rpm for 5 minutes, resuspended in 1 mL of media, and counted using the hemocytometer. After calculating the total cell number, the hMSCs were seeded in different containers appropriate for corresponding in vitro experiments.

Live/Dead Assay

Biosurfaces, Inc. was responsible for making the electrospun scaffold used in viability testing. The protocol for the test was developed by Nancy Duffy, a past graduate student in the WPI Myocardial Regeneration lab. The purpose of the test is to determine and demonstrate hMSC viability and attachment on the electrospun scaffold. As preparation for cell seeding, the scaffold was cut into 6 mm by 6 mm squares and place in a 98 well plate to be sterilized by Ethylene Oxide (EtO) gas as shown in the figure below.

96 well plate containing 4 6 mm by 6 mm sheets of the electrospun scaffold after EtO gas sterilization.

Following the established protocol, 100 mL of cell suspension containing 200,000 hMSCs were added to each well with the scaffold. To ensure optimal attachment of the cells on the scaffold, the wells were checked to ensure that no scaffold was floating on top of the cell suspension. In addition, 100 mL of cell suspension with 50,000 hMSCs were added to two empty wells for controls. The growth media was changed the day after seeding and every other day afterwards.

After seven days, the cells were stained with live/dead staining to determine their viability on the electrospun scaffold. The proper concentrations of Ethidium Bromide and the fluorescent dye calcein were provided by Chirantan Kanani. The mixture solution of the two dyes was prepared by adding 2 µL of Ethidium Bromide and 0.5 µL of calcein in 1 mL of sterile serum-free DMEM. Then, the wells containing the cells were washed with PBS while ethanol was added to one of the plastic wells to create a negative control. After each well was aspirated, the live/dead solution was added and incubated for 15 minutes at 37 °C. The plate was imaged immediately afterwards and the resulting images can be seen below.

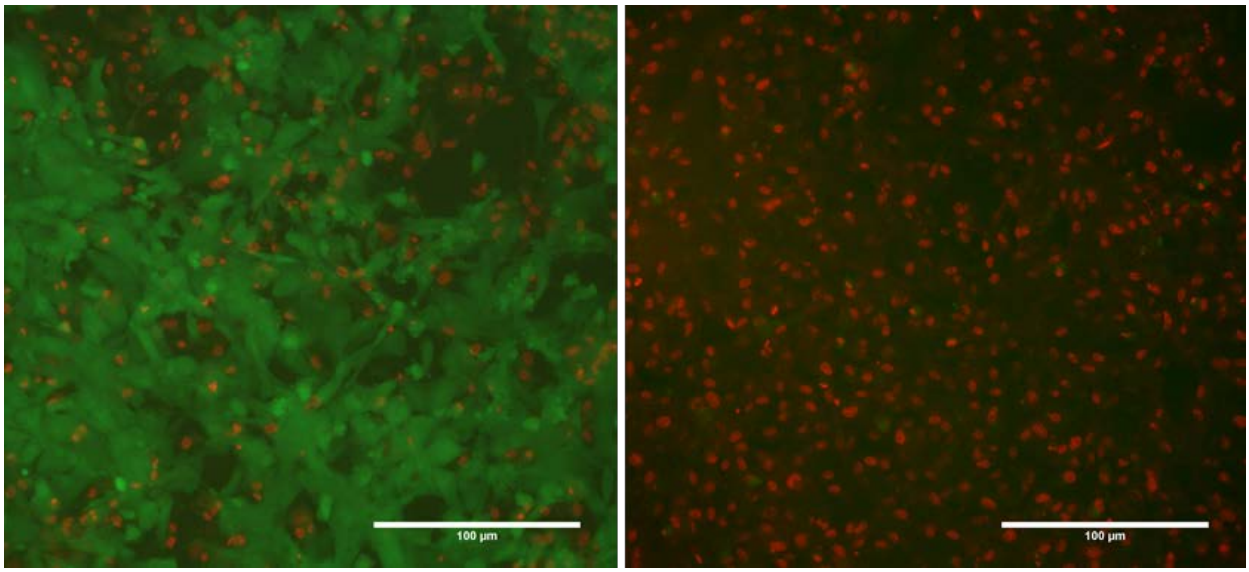

Positive (left) and negative (right) controls of the live/dead stain on hMSCs after 7 days of culturing.

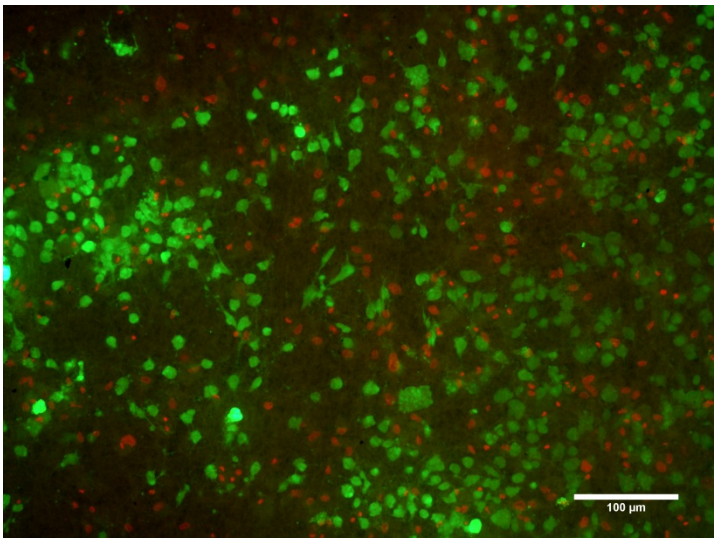

Live/dead stain of hMSCs on electrospun scaffold at day 7.

As shown in figure 5.13, the experiment demonstrated the effectiveness of the staining in identifying non-viable cells. The negative control treated with ethanol showed only red signal, which is an indication of non-viable cells. In comparison, a green signal was detected in the positive control and the experimental sample indicating the presence of viable cells. However, the prevalence of non-viable cells in the positive control raised some serious concerns. It was proposed that future viability testing would be performed on cells cultured for 24 hours after seeding. Additionally, cell morphology will be examined while the cells are attached to the scaffold in order to determine the effects that the material has on the cells.

Appendix B: Objectives Tree

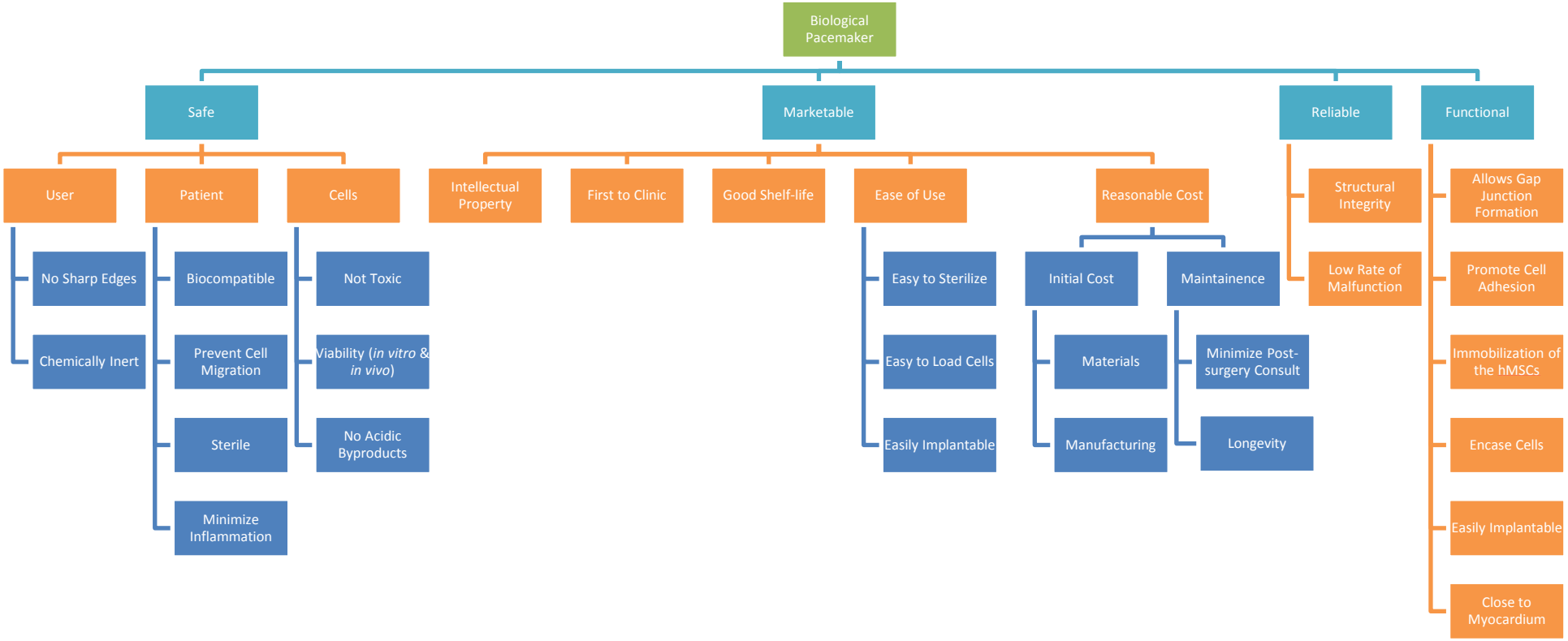

Appendix C: Function Means Tree